LONGITUDINAL SHEAR CAPACITY OF THE SLABS OF COMPOSITE BEAMS

-o0o-o0o-o0o-o0o-

LONGITUDINAL SHEAR CAPACITY OF THE SLABS OF COMPOSITE BEAMS

by

MOHAMMED NAEL EL-GHAZZI, B.Civil Eng.

A Project Report

Submitted to the Faculty of Graduate Studies

in Partial Fulfilment of the Requirements

for the Degree

Master of Engineering

McMaster University

November 1972

MASTER OF ENGINEERING (1972) McMaster University

(Civil Engineering) Hamilton, Ontario

TITLE: Longitudinal Shear Capacity of the Slabsof Composite Beams.

AUTHOR: Mohammed Nael El-Ghazzi, B.Civil Eng., University of Riyad, Saudi Arabia.

SUPERVISOR: Professor H. Robinson

NUMBER OF PAGES: xii, 88

SCOPE AND CONTENTS:

In this report, a method for calculating the longitudinal shear capacity of the slab of simply-supported steel-concrete composite beams is presented. The method is based on analysing the stresses at failure of the concrete elements located at the slab shear surface. In this analysis, the slab width and the shear span are found to be two main parameters that have been neglected inthe empirical solutions previously adopted.

A C K N O W L E D G E M E N T S

The author wishes to express his sincere thanks and appreciation to Professor H. Robinson for his advice and guidance received during every stage of the progress of this report.

The author is also grateful to the Department of Civil Engineering and Engineering Mechanics for providing a teaching assistantship.

The investigation was supported by a grant from the Canadian Steel Industries Construction Council.

TABLE OF CONTENTS

NOTATION

A_{cc}	the longitudinal shear area of concrete per connection.
A_{rc}	total area of transverse reinforcement per connection.
A_s	area of steel beam section
A_t	total area of transverse reinforcement per unit length of slab.
a	depth of concrete compression zone
b	width of concrete slab
b'	thickness of push-off specimen
C	concrete compressive force in the slab
C'	compressive force acting at the steel area subjected to compression
d	depth of steel beam
d'	length of push-off specimen
E	Elastic modulus of steel lever arm between compressive force, C, and tensile force, T.
e'	lever arm between compressive force, C', and tensile force, T.
F_y	steel beam yield strength
f'_c	concrete cylinder strength at 28 days
f_y	yield stress of transverse reinforcement
h	height of the cellular part of slab
K_1, K_2	the concrete and reinforcement coefficients respectively as used in the empirical approach.

L	beam span
L_s	length of shear surface at the shear connection
L_v	shear span
eM_c	experimental moment at first visible longitudinal cracking
eM_u	experimental ultimate moment of resistance
tM_u	theoretical ultimate moment of resistance
m	number of shear connections in the shear span
n	number of times each longitudinal shear reinforcing bar is intersected by a shear surface
p	transverse steel ratio in slab
p'	transverse steel ratio for the case of partial flexural capacity
$(p)_u$	transverse steel ratio for the case of full flexural capacity
$(pf_y)_u$	transverse stress produced by transverse slab reinforcement for the case of full flexural capacity
p_b	transverse steel ratio in the tensile zone of the slab
p_t	transverse steel ratio in the compressive zone of the slab
Q	shear force in a shear connection
Q_c	shear force in a shear connection at first longitudinal cracking

Q_u	shear force in a shear connection at ultimate capacity
eQ_u	experimental shear force in a shear connection at ultimate capacity
tQ_u	theoretical shear force in a shear connection at ultimate capacity
S	longitudinal spacing of shear connections
T	tensile force in steel beam
t	effective thickness of slab
U_w	cube strength of concrete
V	applied force in push-off specimen
v	longitudinal shear stress
v_u	longitudinal shear stress at ultimate load
v_c	shear stress on a concrete element in the compression zone of the slab
v_t	shear stress on a concrete element in the tensile zone of the slab
w	width of push-off specimen
σ	normal stress
σ_x	transverse normal stress
σ_y	longitudinal normal stress
θ	the inclination to the horizontal axis of the line passing through the origin and the point (σ_y, v)
ϕ	principal direction at failure

ϕ_c principal direction at failure for the elements of the compression zone of the slab

ϕ_t principal direction at failure for the elments of tensile zone of the slab

α ratio of the longitudinal normal compressive stress to the specified concrete compressive strength

α_{min} the value of α when the transverse normal stress is zero

α_u the value of α when the transverse normal stress is $(pf_y)_u$

β ratio of the longitudinal normal stress to the concrete tensile strength

ρ ratio of the shear stress v_c in the compression zone of the slab to the shear stress v_t in the tensile zone of the slab.

LIST OF FIGURES

LIST OF TABLES

CHAPTER I

LONGITUDINAL CRACKING

The exact magnitude and distribution of stresses which are present in practice in a composite floor system incorporated in a building is extremely difficult to determine. However, most tests which have been done to study the longitudinal shear strength and the effect of transverse slab reinforcement were made on simply supported beams with a point load at midspan.[3][4]* For such cases the stresses present in the concrete slab can be classified into two groups, depending on their effect. The first group of stresses has a major effect on the behaviour of the beam, and these stresses, usually, determine the ultimate load-carrying capacity of the composite beam. These stresses include:

1. bending stresses (tension and compression) as a result of the steel-concrete interaction.
2. longitudinal shear stress which is produced by the action of the shear connectors.

The second group of stresses includes:

1. transverse bending stress and vertical shear due to the dead weight of the slab.
2. local compressive stresses in the concrete at the root of the shear connectors.

---

*Number in parenthesis refers to the reference listings.

In general, the effect of the second group of stresses is small, as a result of which they have been neglected in design and analysis.

The longitudinal shear stress at a section along the line of the shear connectors is dependent upon the horizontal shear force, Q, in the adjacent connector. For the case of a simply supported beam with a point load at mid span, the shear force is assumed to be the same for all the connectors. However, the magnitude of the shear force, especially in the inelastic range, tends to a maximum at the vicinity of the load point. Figure (1.1) shows a typical shear force diagram for a simply supported beam with constant spacing of shear connectors.[4] In fact, the shear force distribution along the beam is a function of the slip between the steel beam and the concrete slab, therefore the Q diagram shown also represents the slip variation along the beam.

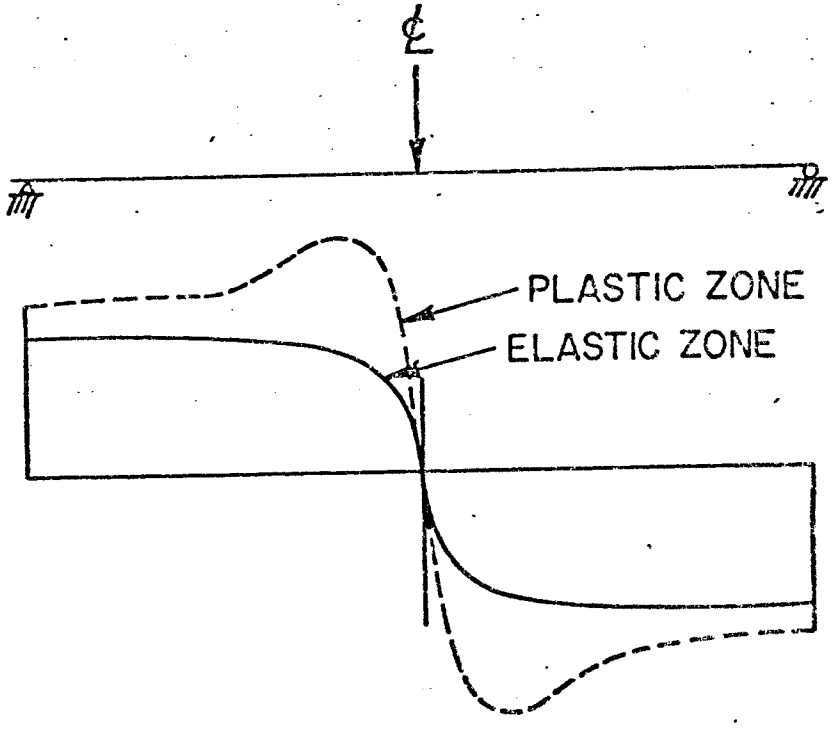

FIG.(1.). TYPICAL SHEAR FORCE DISTRIBUTION ALONG THE SPAN OF A SIMPLY SUPPORTED BEAM

All previous design methods have considered constant longitudinal shear stress through the slab thickness which is equal to the shear force, Q, in a connector divided by the shear plane (equal to L_sXS). This assumption implies that the shear strength is the same in the upper and lower parts of the concrete slab. Since in all beam tests, as well as in practice, the top part of the slab is in compression whereas the lower part is in tension, the previous assumption neglects the effect of bending stress on the ultimate shear capacity of the slab. However, Davies[3] and the CP117[1] design method recommend that the transverse reinforcement should be placed in the lower part of the slab in order to account for the harmful effect of the flexural tensile stress on shear strength of the slab.

Longitudinal cracking along the line of the shear connectors may occur if the slab fails to resist the longitudinal shear stress produced by the connectors. The crack development is thought to be due to excessive principal tensile stress. Therefore, a plain concrete slab will fail when the produced principal tensile stress is equal or greater than the concrete tensile strength which is proportional to the square root of the compressive strength.[8] If transverse reinforcement is provided, the cracking resistance of the slab will be improved such that the crack starts when the yield stress of the reinforcement is

reached.[3] Thus, a certain amount of reinforcement has to be used in order to prevent excessive longitudinal cracking of the slab and to achieve the maximum load-carrying capacity of the composite beam.

Longitudinal cracking usually starts near the point load in a test beam at which the dual action of bending and shear stresses is a maximum. It is thought[3][1] that the crack starts in the lower part of the slab then propagates to the upper part to become visible. This behaviour has been reasoned by the fact that axial tension causes a decrease in the diagonal tension strength while axial compression increases it. Once the crack starts, it then develops towards the supports as the load increases. As a result of the crack development towards the supports, a greater loss of interaction between the concrete slab and the steel beam is expected to occur, thus cutting down the load-carrying capacity of the beam. Davies showed that the progress of the longitudinal crack towards the supports is dependent upon the amount of transverse reinforcement present in the slab. The lower the transverse reinforcement parameter, pf_y, the lower the percentage of theoretical ultimate flexural capacity at which cracks first form and the more rapidly they extend towards the supports. The development of longitudinal cracks can be considered to constitute a type of failure which must be taken into account in the ultimate strength analysis of composite beams.

CHAPTER II

EXISTING DESIGN PROCEDURE

2.1 General

Neither the CISC[5], AISC[6] nor ACI[7] specifications makes any reference to longitudinal shear stress or transverse reinforcement in the concrete slab of a composite beam. Thus, the reinforcement is left to be determined solely by the transverse bending moment in the composite floor slab. This means that in case of small or zero transverse moment, as in most composite tests, there will be no apparent need for slab reinforcement. For such cases, it was shown by Davies that only 50 to 60 per cent of the capacity of the composite beam would be achieved without transverse reinforcement.

In the following sections, the existing design methods and equations are mentioned and discussed.

2.2 C.P. 117:1965 Design Equations

The British Code of Practice CP 117, Part I[1] does cover the longitudinal shear strength of composite beams with solid or hunched slabs, but it was written in 1964 when only a few beams had been tested. However, there is evidence that the C.P. 117 Equations give a considerably conservative estimate of the required transverse reinforcement as compared to Davies'[3] results.

The CP 117:1965 design equation states that:

The shear force (lbf) per inch run of beam, $\frac{Q_u}{S}$, should not exceed either

1. the shear resistance per inch run of beam which is equal to:

$$2.8\ L_s\sqrt{U_w} + A_t f_y\ n \qquad \ldots (2.1)$$

or

$$7.5\ L_s\sqrt{U_w} \qquad \ldots (2.2)$$

Furthermore, the amount of transverse reinforcement A_t to be placed entirely in the bottom of the slab or haunch should not be less than:

$$\frac{Q_u}{4Sf_y}\ \text{in}^2 \text{ per inch run of beam} \qquad \ldots (2.3)$$

Equations (2.1) and (2.2) can be rewritten in terms of cylinder compressive strength, f_c', instead of U_w to be in the form of equations (2.4) and (2.5) respectively.

$$\frac{Q_u}{S} \leq 3.5\ L_s\sqrt{f_c'} + A_t f_y\ n \qquad \ldots (2.4)$$

and

$$\frac{Q_u}{S} \leq 10\ L_s\sqrt{f_c'} \qquad \ldots (2.5)$$

where,

L_s = the length of the shear surface at the shear connectors, in inches, but not to be taken to be

more than twice the slab thickness.

n = number of times each lower transverse reinforcing bar is intersected by a shear surface. Generally, for T-beams, n = 2 and for L-beams n = 1.

It should be stated here that the following assumptions were made in the previous CP 117 Equations:

1. The development of the longitudinal crack in the slab is mainly due to excessive principal tensile stress.
2. The resistance of concrete to principal tensile stress is directly proportional to the square root of the cylinder strength. In fact the concrete terms in equations (2.1) and (2.4) are derived from ACI - ASCE committee 326[8] recommendation that the ultimate diagonal tension strength of an unreinforced web shall not exceed $3.5\sqrt{f'_c}$, which in terms of cube strength is $2.8\sqrt{U_w}$. Similarly, equation (2.2) is derived from the same recommendation that the safe upper limit for shear stress is given by $8\sqrt{f'_c}$ or $10\sqrt{f'_c}$ depending upon the shape of the cross-section of the concrete.
3. The reinforcement contribution in resisting longitudinal shear is proportional to the yield stress of reinforcing bars. The reinforcement term in equation (2.1) considers that a crack will certainly develop in the

concrete when the yield stress of the reinforcement is attained.

4. The reinforcement in the upper part of the concrete slab is not considered to be effective in resisting longitudinal shear and the proposed reinforcement is in addition to that required to resist transverse bending of the slab.
5. Neither the longitudinal bending nor the width or length of the slab have been taken to have any effect on the longitudinal shear strength of the concrete slab.

2.3 Johnson Design Method and Approach

In his paper "Longitudinal shear strength of composite beams" Johnson[2] has recommended a new ultimate design method for the transverse reinforcement in the solid slab of a composite beam. He studied all available results of tests to failure on positive and negative moment regions of composite beams with and without negative transverse bending of the slab including over 60 beams at Cambridge University. His design method makes use of the following conclusion which he had found from his study.

1. All transverse reinforcement contributes to longitudinal shear strength, irrespective of its level in the slab and of the magnitude of the negative

transverse bending moment.

2. No account need be taken of longitudinal bending (of either sign) in determining the longitudinal shear strength of a composite beam.

Johnson has found that the shape and dimensions of the composite beam affects the required amount of reinforcement. He stated that the value of pf_y for a given shear stress, v_u, depends on the shape coefficient of the beam which is essentially the ratio of the slenderness of the beam to that of the slab forming its top flange. He also reported the effect of the shape coefficient, λ, to be as shown in Fig. (2.1). Nevertheless, he neglected the effect of λ in his design equations on the base that the practical range of λ was found to between 0.7 and 1.4.

Johnson's design method proposed the following:

The total amount of transverse reinforcement should satisfy

$$pf_y \geq 1.26\, v_u - 3.8\sqrt{f'_c} \qquad \ldots (2.6)$$

$$\geq 80 \quad \text{psi} \qquad \ldots (2.7)$$

and the reinforcement should be placed in the slab such that:

$$p_b f_y \geq \tfrac{1}{2}\, pf_y$$

$$p_t f_y \geq \tfrac{1}{2}\, pf_y$$

$$\geq \text{the reinforcement required to resist negative transverse bending of the slab} \qquad \ldots (2.8)$$

where v_u = the mean ultimate longitudinal shear stress on a possible plan of longitudinal shear failure.

and p_b and p_t = the transverse reinforcement per unit area present at the bottom and top of the concrete slab, respectively.

Almost the same assumptions as well as the variable parameters used in CP 117 design equations have been used by Johnson, resulting in a reasonable similarity between the two designs. The main two differences between CP 117 and the Johnson design equations are the reinforcement and concrete coefficients and the placement of the reinforcement in the slab.

For comparison purposes, the two previous design equations as well as Davies' are represented graphically in Fig. (2.2). Davies work and approach are discussed in detail in Chapter IV.

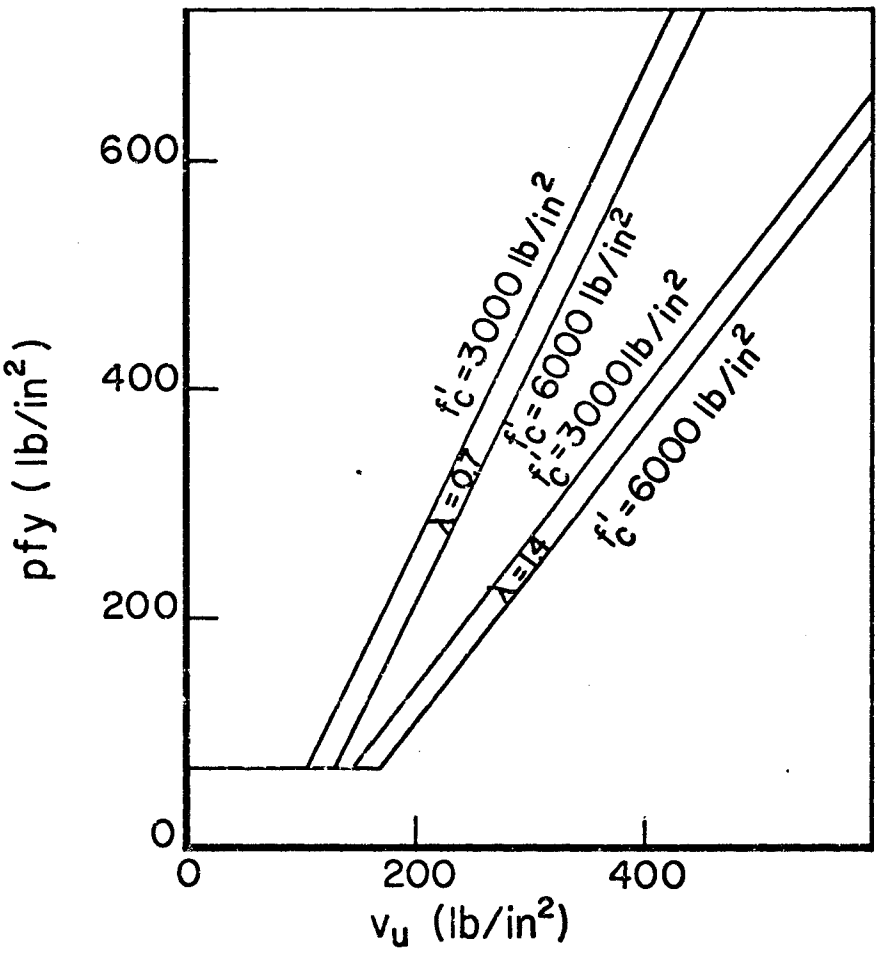

FIG. (2.1) - JOHNSON DESIGN METHOD; EFFECT OF THE SHAPE COEFFICIENT, λ, ON THE TRANSVERSE REINFORCEMENT IN COMPOSITE BEAMS UNDER DISTRIBUTED LOADING.

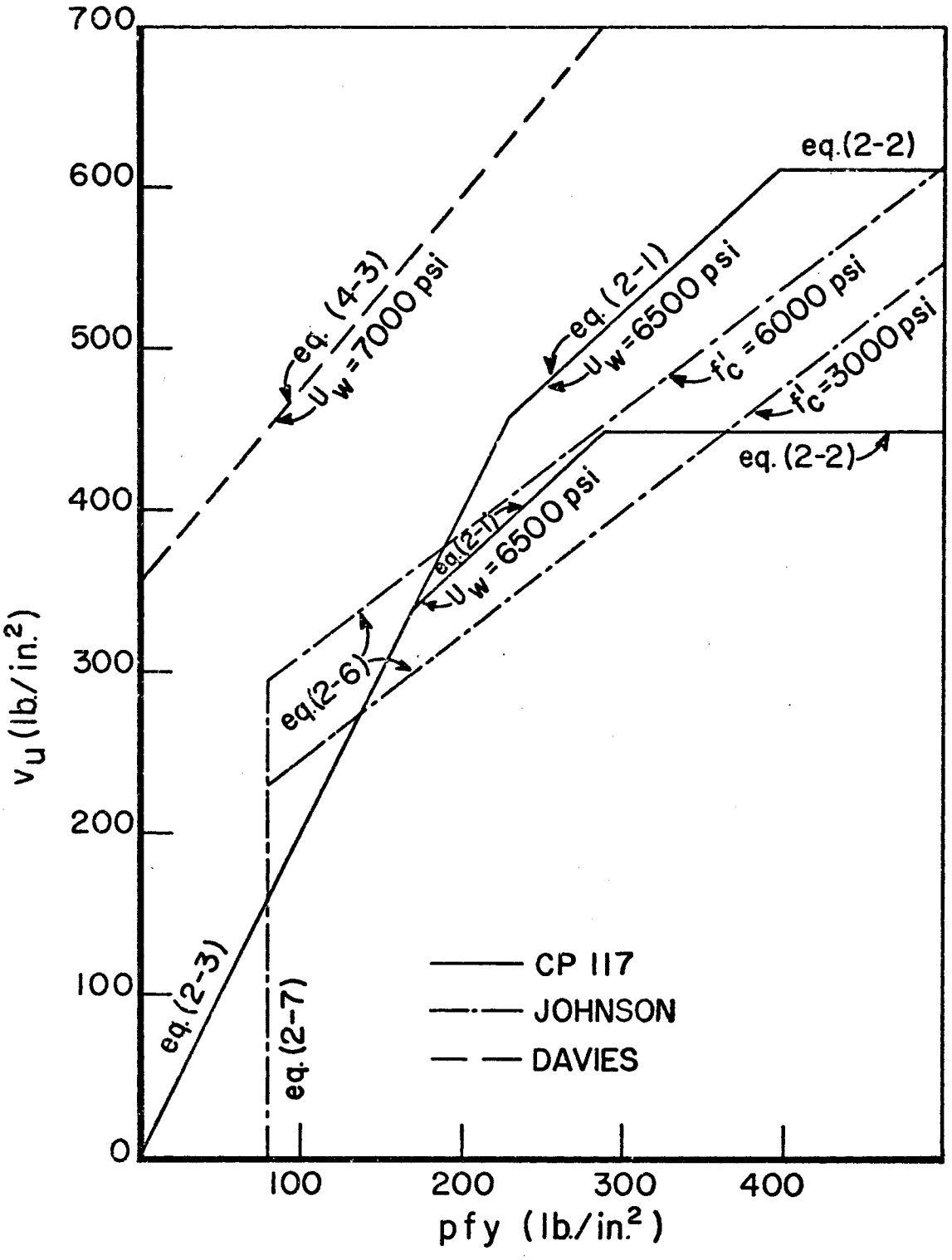

FIG. (2.2) - GRAPHICAL REPRESENTATION OF THE EXISTING DESIGN EQUATIONS.

CHAPTER III

TESTS ON COMPOSITE BEAMS INCORPORATING 3 - in. CELLULAR DECKING

3.1 General

For composite steel-concrete beams having a solid slab it has been demonstrated experimentally that slip between the steel beam and the concrete slab is small, resulting in the effect of slip being neglected and the composite beam considered as having full interaction. However, with a composite beam incorporating cellular metal decking the cellular zone constitutes a much more flexible zone between the solid part of the slab and the steel beam, and in which larger slip can occur, resulting in some loss of interaction. In addition, the cellular metal deck as well as the geometry of the concrete ribs present more difficulties in predicting the overall behaviour and the stresses acting in the solid part of the slab. Therefore, it is expected to see some differences in the behaviour and performance of the two previous types of composite beam as far as longitudinal shear strength of the slab is concerned.

Most test results available to date have considered the ultimate capacity of the composite beam without detail or any reference to the behaviour and performance of the

beam at the start of longitudinal cracking. Davies has studied the stage of first cracking in enough detail, and his tests on solid slab composite beams as well as his empirical approach are discussed in the following chapter. Three composite beams incorporating cellular metal decking which have been tested are reported in this chapter with an emphasis on the stress conditions at first visible longitudinal cracking.

The tests reported herein were originally made to study the ultimate capacity and performance of the type of beam in question. The experimental work consisted of three simply supported beams of different span length and slab width which were loaded to failure by a single point load at mid-span.

3.2 Description of Beams:

The identification of the beams used herein is as follows: the numerator and denominator of the subscripted ratio denote the width and span length in feet of the concrete slab respectively. Thus $B_{8/30}$ designates the beam having 8 ft. slab width and 30 ft. span length.

All the beams tested had the same amount and type of transverse reinforcement, steel beam, metal deck and shear connectors. Description and properties of the beams are summarized in Table (3.1), whereas detailings and dimensions are shown in Fig. (3.1). The transverse

reinforcement of the beam was provided by using 6 x 6, 10/10 welded wire mesh placed approximately at mid-depth of the solid part of the slab. The mesh wires are 0.135 - in. in diameter resulting in 0.0143 $in.^2$ cross-sectional area and placed at 6 - in. centres in both transverse and longitudinal directions. Based on 0.2 per cent proof stress, the yield stress of the wires, as given by the producer, was 64,000 psi. Since this stress is greater than the upper limit recommended by the British Code of Practice CP117[1], so 60,000 psi was taken to be the yield stress of the transverse reinforcement used in the beams.

Although the steel beams were all from a single rolling, difference in the yield stresses, F_y, were recorded. Four test samples taken from the web and the flanges of each beam were tested for the yield stress and the average of the four values was considered. The term A_sF_y of each beam was calculated from the sum of the areas of the flanges and the web multiplied by the corresponding yield stress.

The metal deck used in the beams was 22 gauge. The concrete ribs of the slab formed by the cellular deck were 2-1/8 in. wide at the bottom and 2-3/8 in. at the top with 2-7/8 in. in height and they were at 6 in centres. Headed studs 4-1/2 in. high and 3/4 in. diameter were staggered at the outstanding legs of the steel beam flanges.

TABLE (3.1)

Details and properties of test beams incorporating cellular decking

BEAM	f_c'	CONNECTORS		TRANSVERSE REINF.			STEEL BEAM YEILD STRESS			A_sF_y
		S	m	A_t	p	pf_y	Top flg.	Bot. flg.	Web	
	psi	in.		in^2/in	%	psi	psi	psi	psi	kip
$B_{8/30}$	4,470	6	29	0.0024	0.097	58	48,100	48,100	48,910	428
$B_{10/30}$	4,060	6	29	0.0024	0.097	58	43,510	43,100	43,860	385
$B_{8/40}$	4,470	6	39	0.0024	0.097	58	48,100	48,100	48,910	428

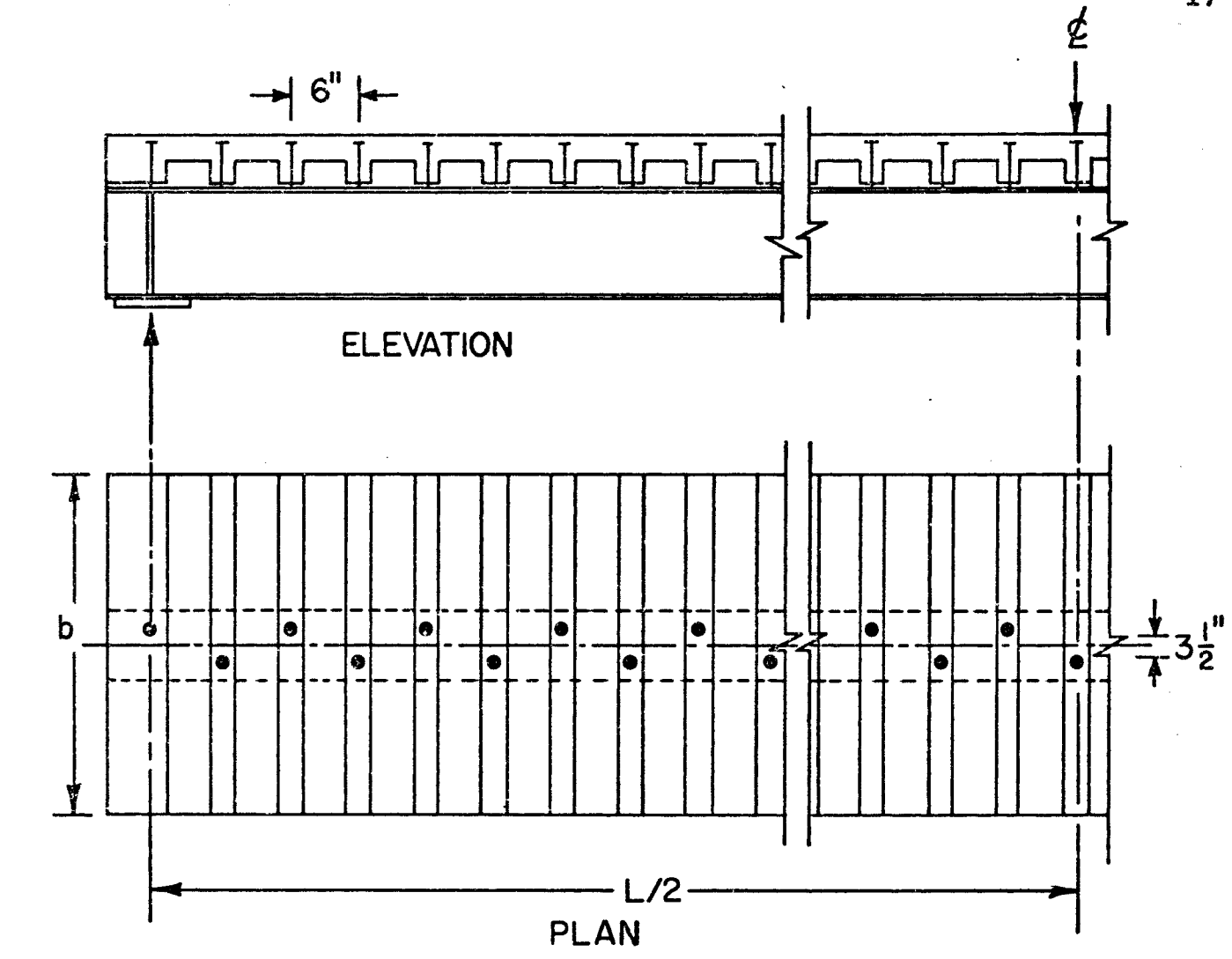

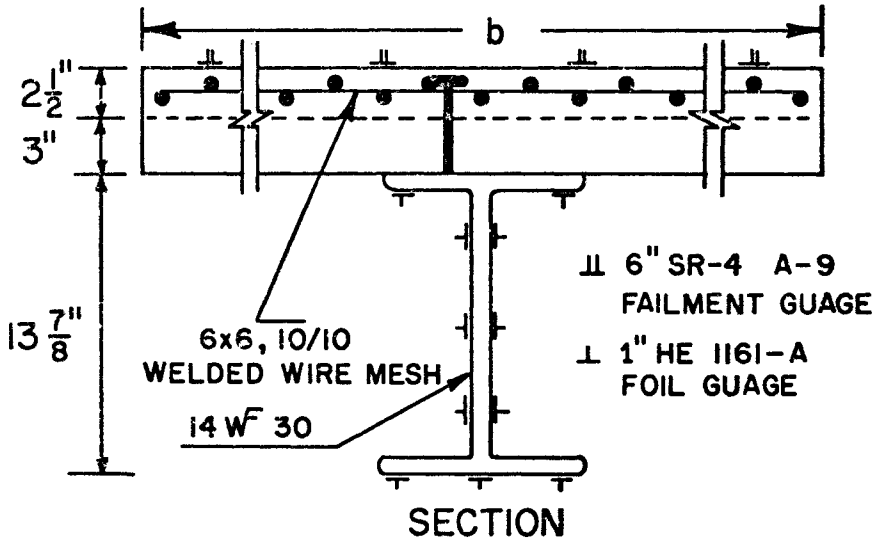

BEAM	b ft	L ft
$B_{8/30}$	8	30
$B_{10/30}$	10	30
$B_{8/40}$	8	40

FIG. (3.1) - GENERAL DETAILS OF BEAMS $B_{8/30}$, $B_{10/30}$ AND $B_{8/40}$.

The studs were placed such that the transverse spacing was 3-1/2 in. and one stud per rib resulted in longitudinal spacing, S, of 6 inches.

The concrete was a commercial ready-mix with a maximum aggregate size of 3/4 in. and a nominal 28 day strength of 3,000 psi. The average crushing strength of concrete cylinders at time of test for each beam as well as other detailings are listed in Table (3.1).

3.3 Instrumentation and Test Procedure

Electric strain gauges were mounted on the steel beam and the top surface of the concrete slab.Fig.(3.1) shows the type and location of the strain gauges used in the tested beams.0.001 in. dial gauges were used to measure the mid-span deflection. Six 0.0001 in. dial gauges, two at the ends of the slab, were mounted to each slab to measure the slip between the top flange of the steel beam and of the concrete slab.

All beams were simply supported and tested to failure with a centre-point load applied by means of a hydraulic jack. The load was applied in 1 kip increments. For each load increment, gauge readings were recorded after a waiting period because a significant relaxation of load occurred.

Strains were measured across the steel beam section at mid-span before and after pouring of the concrete and during

the curing stages to record the dead load and the shrinkage strains.

3.4 Test Results and Analysis

Fig. (3.2) shows the curves of the applied load versus mid-span deflection for the three beams. Also shown in the same Figure are the theoretical load-deflection curves assuming complete interaction, and the stages at which longitudinal and flexural cracks became visible.

The horizontal shear force Q at any stage of loading can be found with reasonable accuracy by means of the strain diagrams across the steel beam section. The strain diagrams for the three tested beams, drawn by means of strain-gauges readings, at first visible longitudinal crack (at point c in Fig. (3.2)) are shown in Fig. (3.3). Knowing the strains, the stress distributions across the steel beam were drawn as shown using a yield-strain value, ε_y, equal to the average yield stress for each beam divided by the modulus of elasticity, E, of steel (29×10^6 psi).

For equilibrium of forces shown in Fig. (3.4) the following equation must be satisfied:

$$T = C + C' \qquad \ldots(3.1)$$

where C is the total compressive force present in the concrete and C' and T are the total compressive and tensile forces present in the steel section respectively.

Thus

$$C = T - C'$$

and since C at a section in between the point of zero and maximum bending moment must equal the sum of the shear forces acting between the section under consideration and the point of zero moment, then

$$C = \Sigma Q_c \qquad \ldots (3.2)$$

Therefore

$$\Sigma Q_c = T - C'$$

or

$$Q_c = \frac{\Sigma Q_c}{m} = \frac{T-C'}{m} \qquad \ldots (3.3)$$

Knowing C' and T for each beam from the stress diagram, then Q_c at first visible crack can be found using equation (3.3). In the calculation made herein, the yield stress and strain for each beam were assumed to be equal in tension and compression, and that the tensile stress in the concrete slab is negligible.

Table (3.2) shows the calculated shear force Q_c and the corresponding longitudinal bending moment at first visible crack as well as the theoretical and experimental ultimate shear force and moments for each beam. The theoretical values of shear and moment were calculated assuming complete interaction between the steel beam and the concrete slab, whereas the experimental values were found by means of trial and error using the partial connection concept.

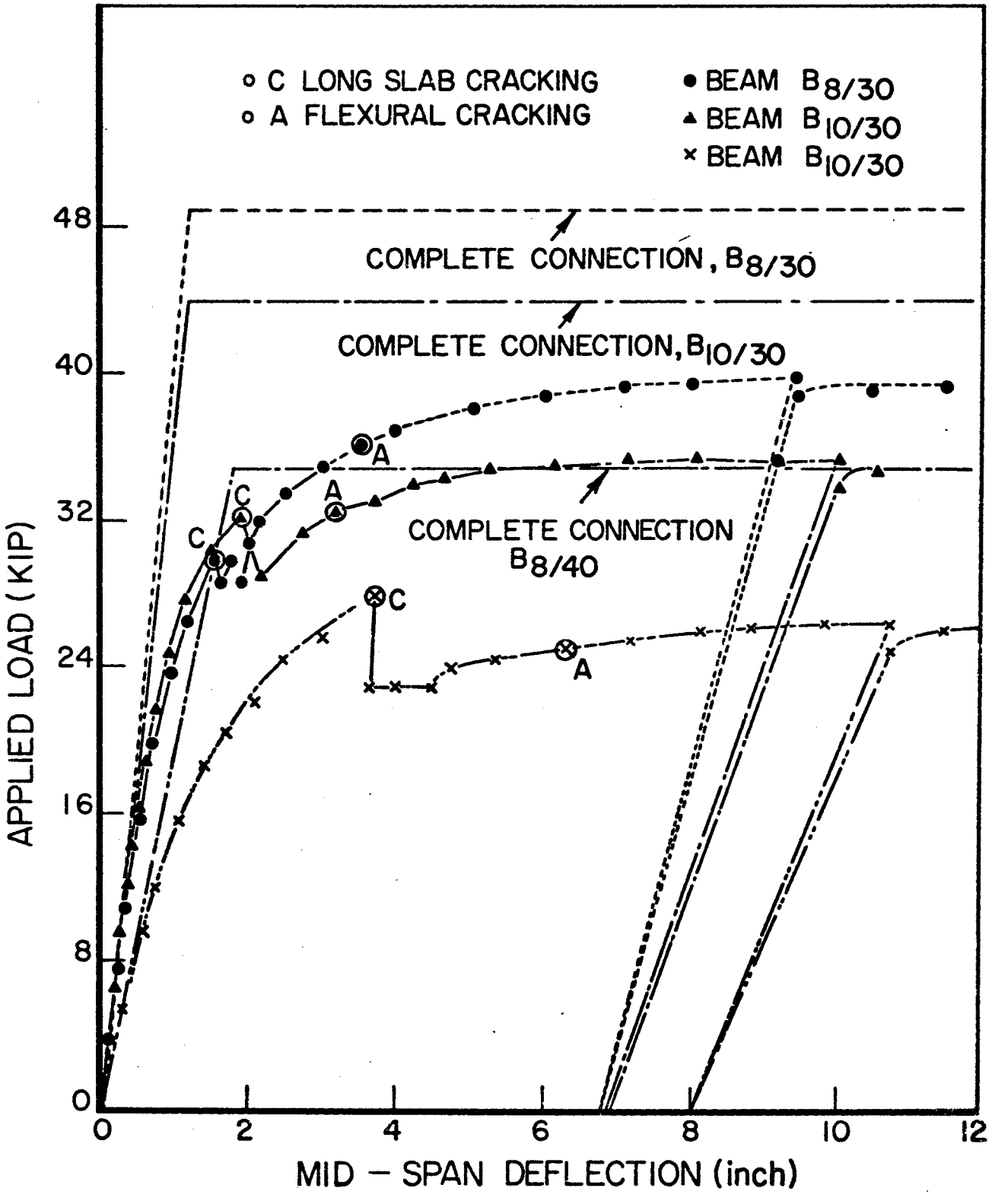

FIG. (3.2) - LOAD-DEFLECTION CURVES FOR BEAMS $B_{8/30}$, $B_{10/30}$ AND $B_{8/40}$.

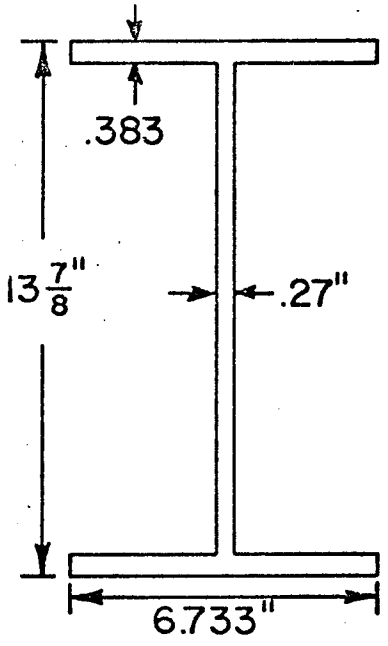

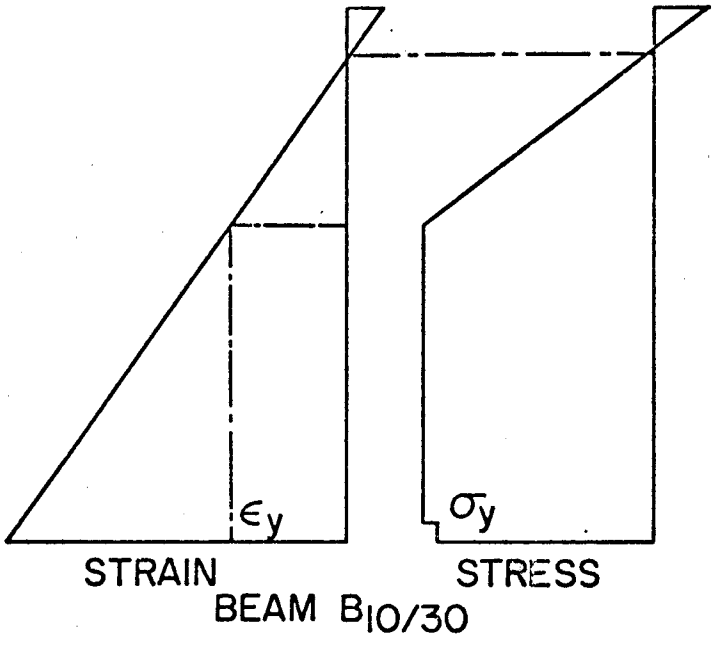

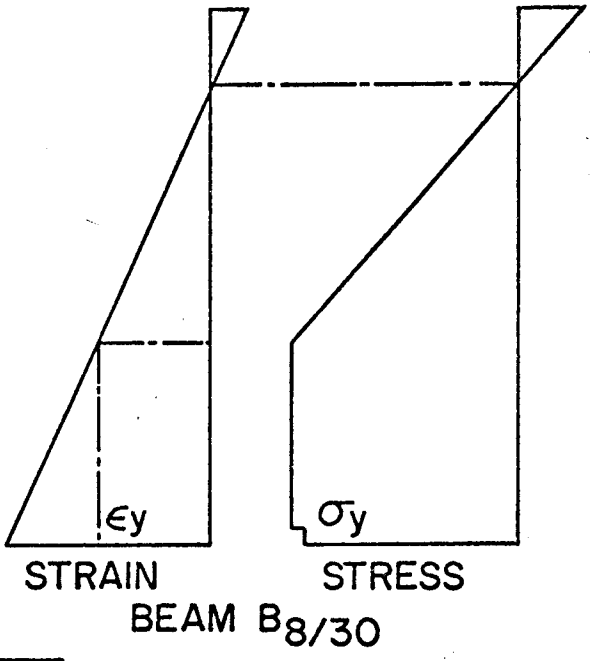

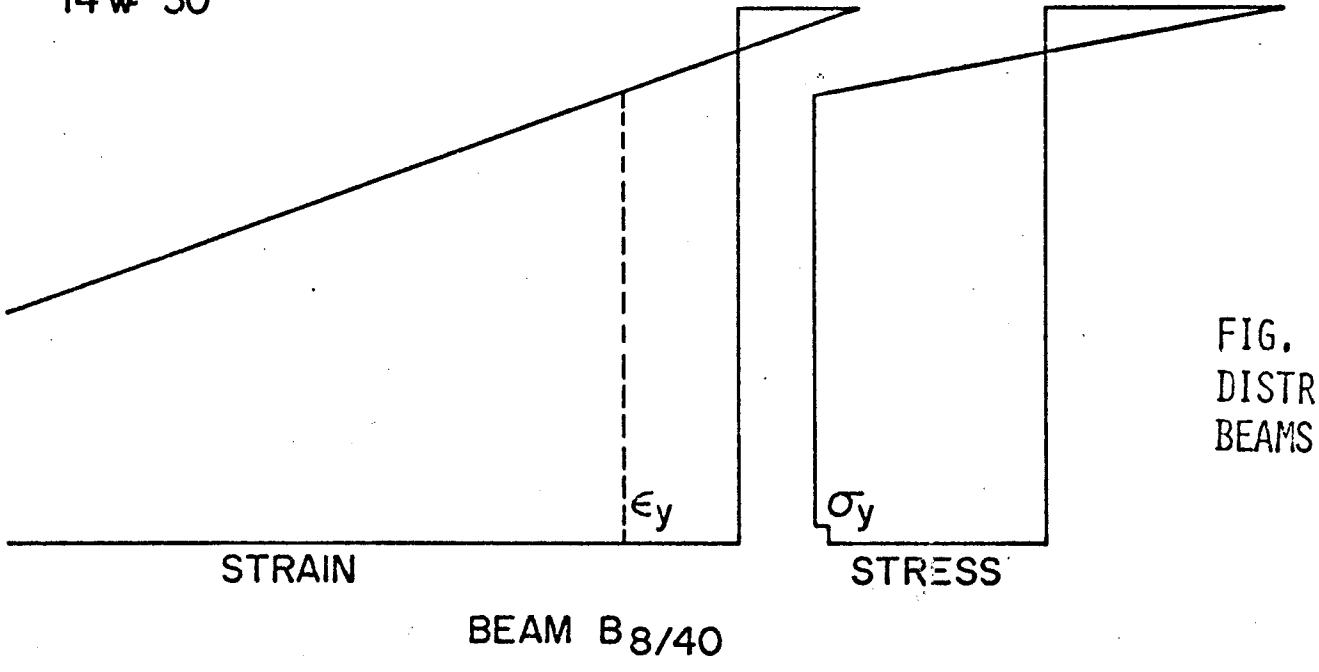

FIG. (3.3) - STRAIN AND STRESS DISTRIBUTIONS IN THE STEEL BEAMS $B_{8/30}$, $B_{10/30}$, $B_{8/40}$.

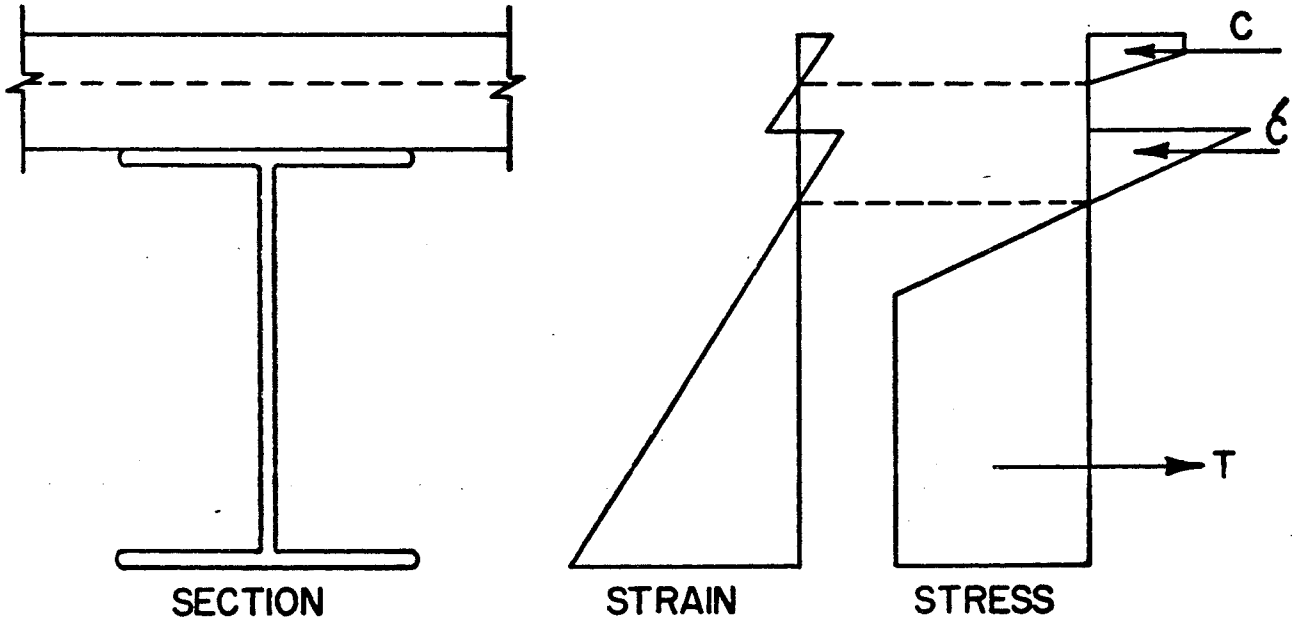

FIG. (3.4) - GENERAL STRAIN AND STRESS DISTRIBUTIONS AT FIRST VISIBLE LONGITUDINAL CRACK.

TABLE (3.2)

Summary of test results

BEAM	Q_c k	eQ_u k	tQ_u k	M_c k.in	eM_u k.in	tM_u k.in	M_c/tM_u	M_c/eM_u	eM_u/tM_u
$B_{8/30}$	6.35	9.15	14.75	3,350	4,170	5,100	0.66	0.80	0.82
$B_{10/30}$	7.0	8.27	13.3	3,590	3,910	4,650	0.77	0.92	0.84
$B_{8/40}$	5.9	5.4	11.0	4,200	4,020	5,100	0.82	1.05	0.97

Fig. (3.5) shows the stress distribution at mid-span section for the two cases: (a) complete connection, and (b) partial connection.

The ultimate strength of the headed studs used in the beams was believed to be more than that required to achieve the theoretical ultimate flexural capacity of the composite beams. None of the beams tested showed any evidence of stud failure or punch out of the rib. All the beams were designed such that the theoretical plastic neutral axis would be within the solid part of the concrete slab. Therefore, the theoretical ultimate shear force for the tested beams would be given by equn. (3.4)

$$\Sigma Q_u = C \quad \text{and} \quad C = T = A_s F_y$$

Then $$\Sigma Q_u = A_s F_y$$

or $$Q_u = \frac{A_s F_y}{m} \qquad \ldots (3.4)$$

and the theoretical ultimate moment would be

$$tM_u = A_s F_y \left(\frac{d}{2} + t + h - \frac{a}{2} \right) \qquad \ldots (3.5)$$

Where $$a = \frac{C}{0.85\, f_c' b} = \frac{A_s F_y}{0.85\, f_c' b} \qquad \ldots (3.6)$$

and t, h is the thickness of the solid and ribbed parts of the slab respectively. d is the depth of the steel beam.

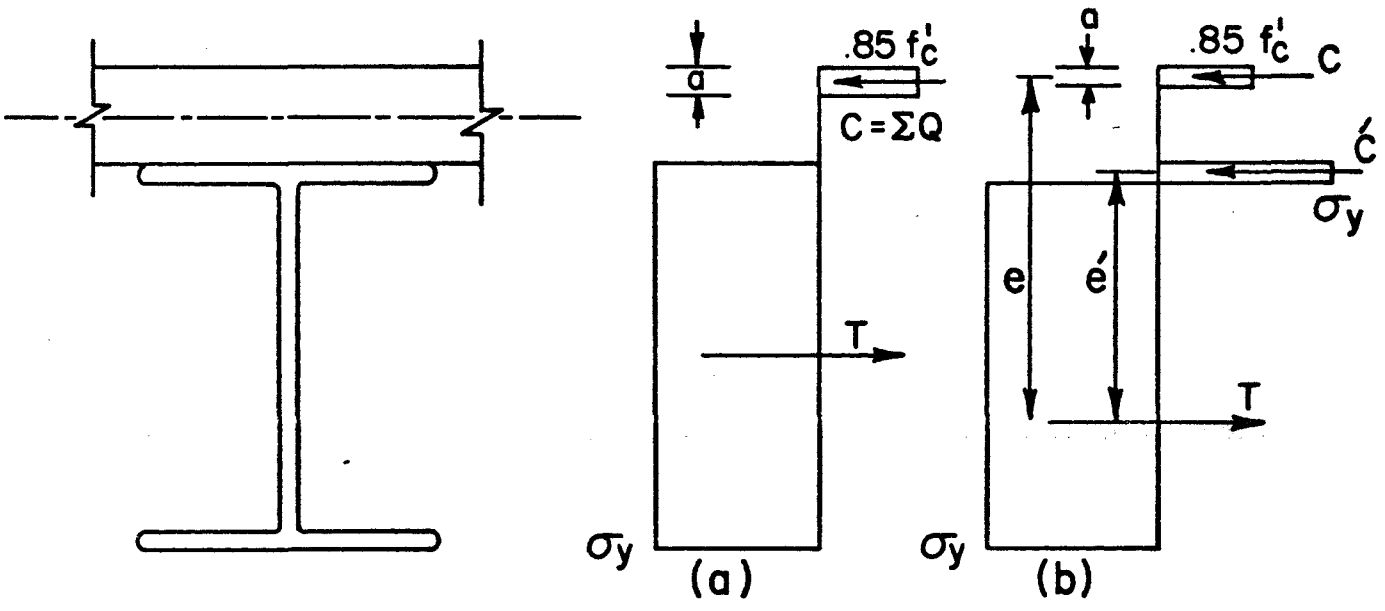

FIG. (3.5) - ULTIMATE STRESS DISTRIBUTION FOR:
(a) COMPLETE CONNECTION.
(b) PARTIAL CONNECTION.

The experimental ultimate moment was found for each beam directly from the ultimate applied load, whereas the corresponding shear force, i.e. $_eQ_u$, was found by solving by trial and error for the forces C and C′ which satisfy force and moment equilibrium. Thus the following equations had been satisfied in finding $_eQ_u$ for the three beams:

for force equilibrium,

$$C + C' = T$$

Substitute $T = A_sF_y - C'$

and rearrange to get $C' = \frac{A_sF_y - C}{2}$ ... (3.7)

and for internal moment equal external moment:

$$M_u = \text{applied moment}$$
$$= C.\,e + C'.\,e' \quad \ldots (3.8)$$

It was shown in Fig. (1.1) that the slip in the in-elastic zone of the composite beam tends to a maximum before or at the vicinity of the point-load. This is also indicated in a composite beam incorporating cellular decking. Fig. (3.6) shows the slip distribution as measured during the loading process of beam $B_{10/30}$. It is clear from the figure that the maximum value of slip has progressed towards the center line of the beam as the load increases and that the equal slip or shear force assumption along

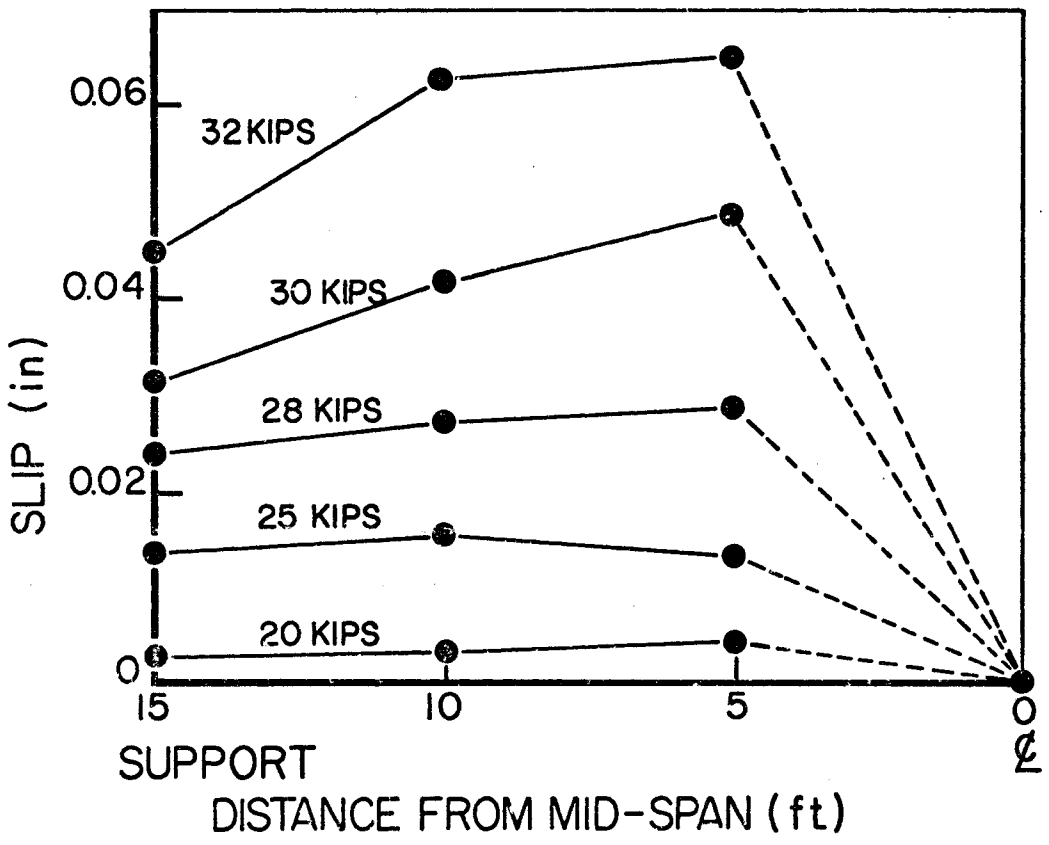

FIG. (3.6) - SLIP DISTRIBUTION ALONG THE SPAN OF BEAM $B_{10/30}$.

the span starts to be violated just before or at the start of longitudinal splitting of the slab.

More discussion of test results and comparison with solid slab composite beam are mentioned in Chapter V.

CHAPTER IV

DAVIES' TESTS AND EMPIRICAL APPROACH

4.1 General

The object of Davies[3] experimental program was to study the behaviour of half-scale composite T-beams when the connector spacing or the amount of transverse reinforcement was reduced in successive beams. He reported in his paper the result of tests on seven steel-concrete composite beams four of which, identified as series 2 beams, were tested to study the longitudinal shear strength.

4.2 Description of Beams and Test Results

All the beams were simply supported and tested to failure at an average age of 35 days by means of a centre point load. The beams had the same cross-section, span length and the same number of identical welded stud shear connectors. The proportion of the beam cross-sections were such that under ultimate load the plastic neutral axis was in the slab. The studs in all the beams were arranged in a single line along the centre of the top flange.

The transverse reinforcement of the slab was provided by means of steel bars 0.212-in. in diameter and having a yield stress of 60,000 psi. Fig. (4.1) and Table (4.1) show

the important details of the beams whereas a summary of the test results is given in Table (4.2). The amount of transverse reinforcement was reduced in successive beams.

The failure of beam A_4, which had the largest amount of transverse reinforcement, was a flexural failure of the slab at mid-span. This was not accompanied by any longitudinal crack along the line of the shear connectors. For the other three beams, longitudinal crack started before achieving the theoretical ultimate moment and the final failure of the beams was accompanied by flexural crushing of the concrete slab at mid-span. In no case was there any failure of the shear connectors themselves.

The moment-deflection curves for the four beams are shown in Fig. (4.2), while the ratios of moments eM_{u/tM_u}, eM_{c/eM_u} and eM_{c/tM_u} are plotted in Fig. (4.3) against the percentage transverse reinforcement. It is clear from the two previous figures that the variation of transverse reinforcement produced a quite definite influence on the capacity of the beams to achieve their ultimate moment of resistance. The eM_{u/tM_u} curve shows that the ultimate moment could be achieved if the amount of transverse reinforcement was equal to or greater than 0.5 per cent. This percentage of reinforcement was considered by Davies to be the minimum that was adequate for the beams tested. In addition, he reported that there would be little, if any, gain of strength for an amount

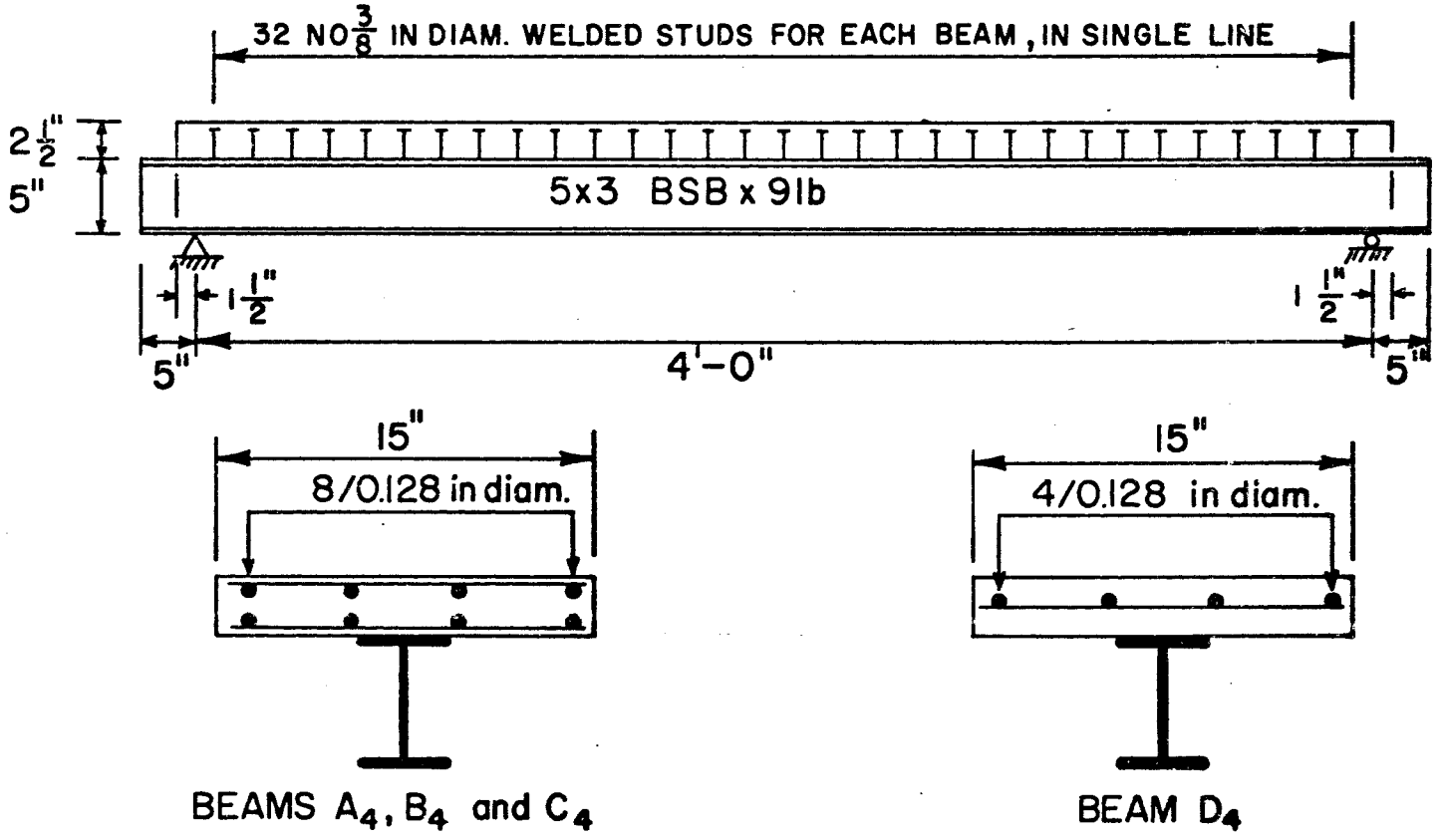

FIG. (4.1) - DETAILS OF BEAMS A_4, B_4, C_4 AND D_4

TABLE (4.1)

Details of beams A_4, B_4, C_4 and D_4

BEAM	U_w psi	CONNECTOR		TRANSVERSE REINFORCEMENT			STEEL BEAM
		S in.	m	A_{rc} in^2/connec.	p %	pf_y psi	$A_s F_y$ kip
A_4	6,200	1.5	16	0.0355	0.94	564	111
B_4	7,300	1.5	16	0.0177	0.47	282	114
C_4	7,300	1.5	16	0.0088	0.235	141	115
D_4	6,500	1.5	16	0.0044	0.118	71	115

TABLE (4.2)

Summary of test results of beams A_4, B_4, C_4 and D_4

BEAM	Q_c kip	eM_c k.in.	eM_u k.in.	tM_u k.in.
A_4	6.92	-	492	455
B_4	5.15	417	485	485
C_4	4.03	362	438	487
D_4	3.14	303	377	474

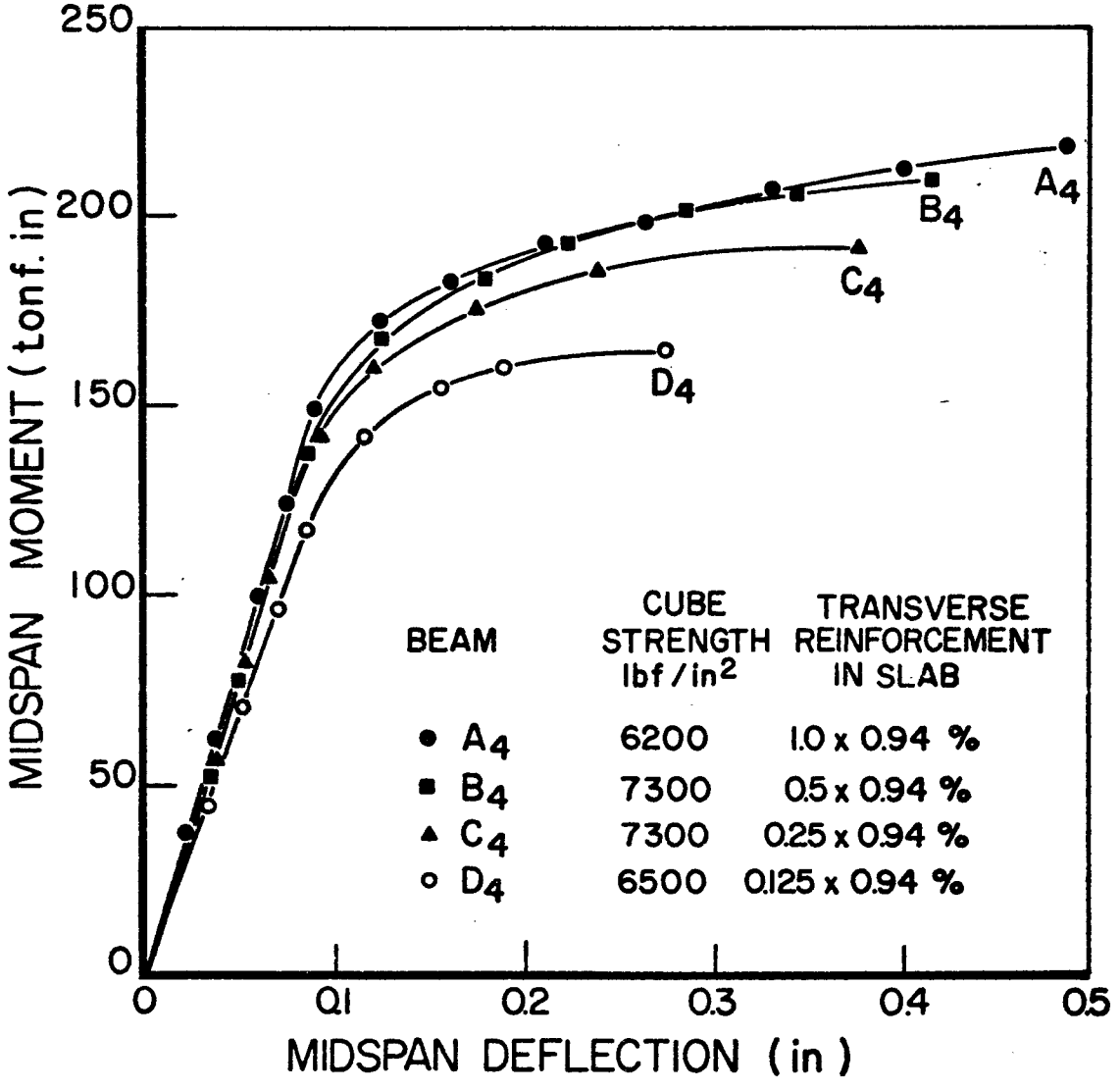

FIG. (4.2) - MOMENT-DEFLECTION CURVES FOR BEAMS A_4, B_4, C_4 AND D_4.

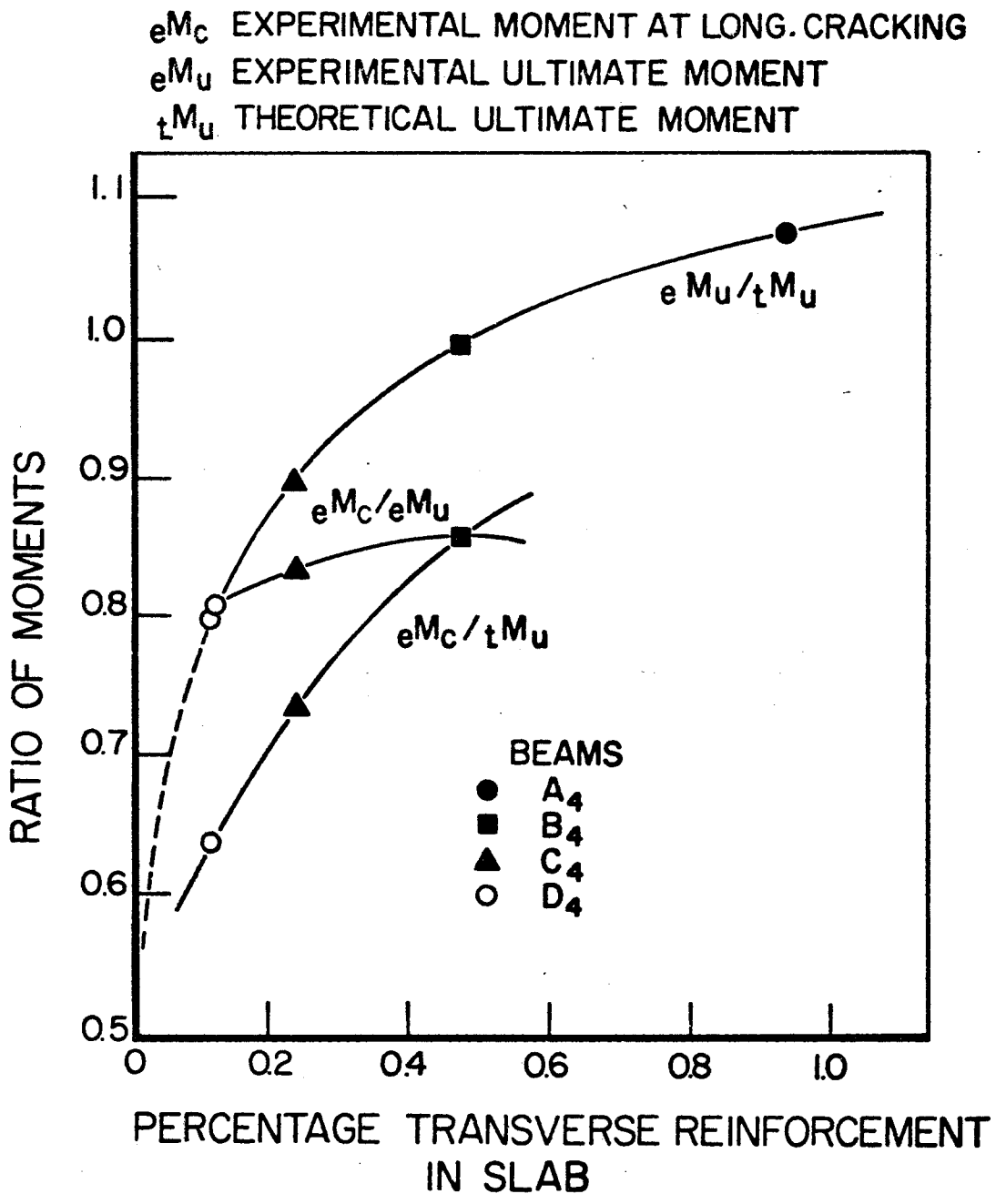

FIG. (4.3) - RATIO OF MOMENTS AGAINST PERCENTAGE TRANSVERSE REINFORCEMENT.

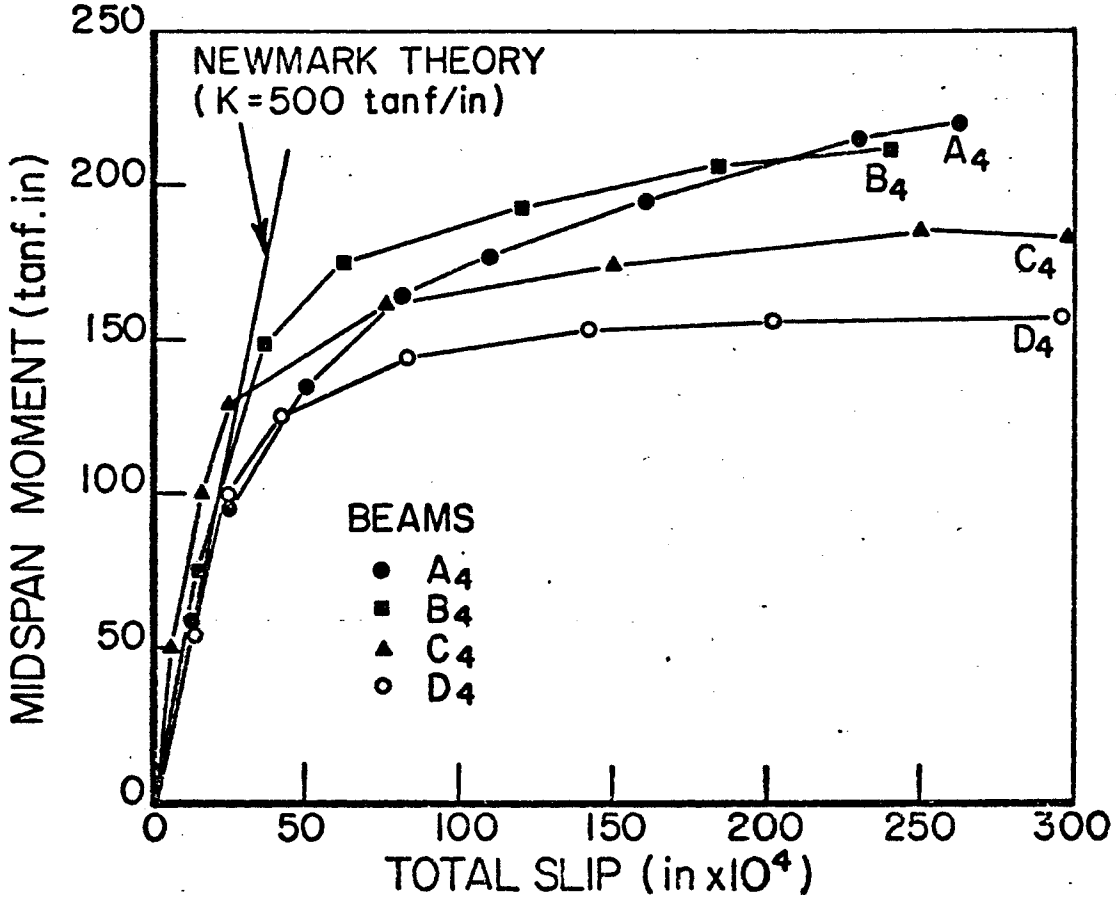

FIG. (4.4) - TOTAL END SLIP FOR BEAMS A_4, B_4, C_4 AND D_4.

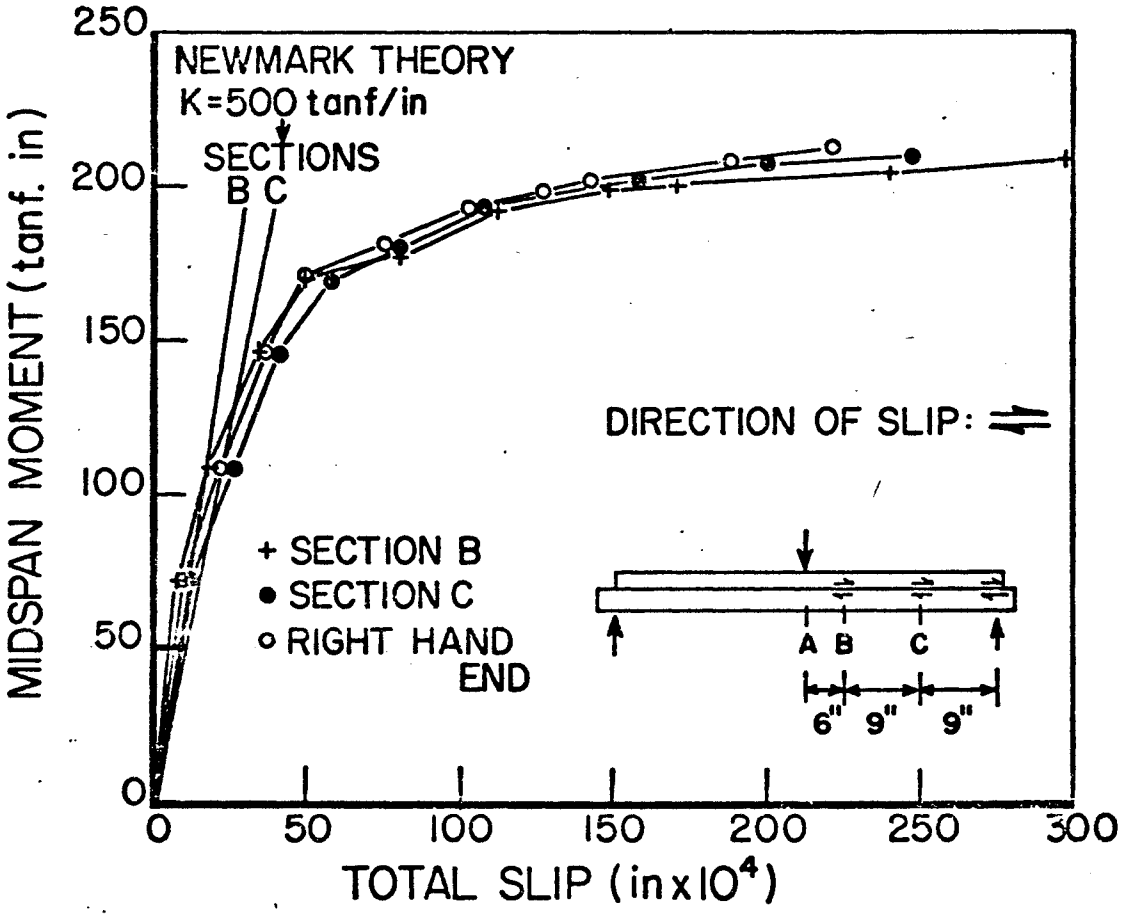

FIG. (4.5) - TOTAL SLIP FOR BEAM B_4.

of reinforcement in excess of 1.0 per cent.

The effect of transverse reinforcement on the amount of slip between the steel beam and the concrete slab is illustrated in Figures (4.4) and (4.5). The first figure shows the total end slip plotted against mid-span moment for the four beams while the second shows the slip variation at different sections along the span of beam B_4.

4.3 An Empirical Approach:

Davies applied the same assumptions as those in the CP 117 design equations when he derived his design equation by using the following empirical approach:

For the case of no transverse negative moment in the slab, the capacity of the slab to resist longitudinal cracking is dependent upon both the concrete and the transverse reinforcement. Therefore, the total resistance of the slab to longitudinal cracking is the sum of the concrete and reinforcement contribution and may be expressed as:

$$\gamma_c A_{cc} + \gamma_r A_{rc}$$

where $\gamma_c = F(U_w)$

$\gamma_r = G(f_y)$

A_{cc} = shear area of concrete per connector

$= t.s$

A_{rc} = total area of transverse reinforcement per connector

$= A_t.S$

The development of a crack is caused by excessive principal tensile stress which can be considered to be comparable to the square root of the cylinder or cube strength of concrete.

Thus $\gamma_c = F(U_w) = K_1 \sqrt{U_w}$

Since a crack would certainly develop in the concrete when the yield stress of the reinforcement is attained, then γ_r can be taken to be proportional to f_y

i.e. $\gamma_r = G(f_y) = K_2 f_y$

where K_1 and K_2 are constants.

Then:

capacity of slab (per connector) to resist ... (4.1)

longitudinal cracking $= K_1 A_{cc} \sqrt{U_w} + K_2 A_{rc} f_y$

Using the experimental data equation (4.1) can be written for each of the beams B_4, C_4 and D_4:

$$\left.\begin{aligned} 5.15 &= 3.75 K_1 \sqrt{7300} + 60{,}000 \times 0.0177 K_2 \\ 4.03 &= 3.75 K_1 \sqrt{7300} + 60{,}000 \times 0.0088 K_2 \\ 3.14 &= 3.75 K_1 \sqrt{6500} + 60{,}000 \times 0.0044 K_2 \end{aligned}\right\} \quad (4.2)$$

From the graphical representation of the above three equations, shown in Fig. (4.6), Davies has selected approximate values for K_1 and K_2 as 8.5 and 2.4 respectively. Then equation (4.1) becomes,

$$Q_c = 8.5 A_{cc} \sqrt{U_w} + 2.4 A_{rc} f_y \quad \ldots (4.2)$$

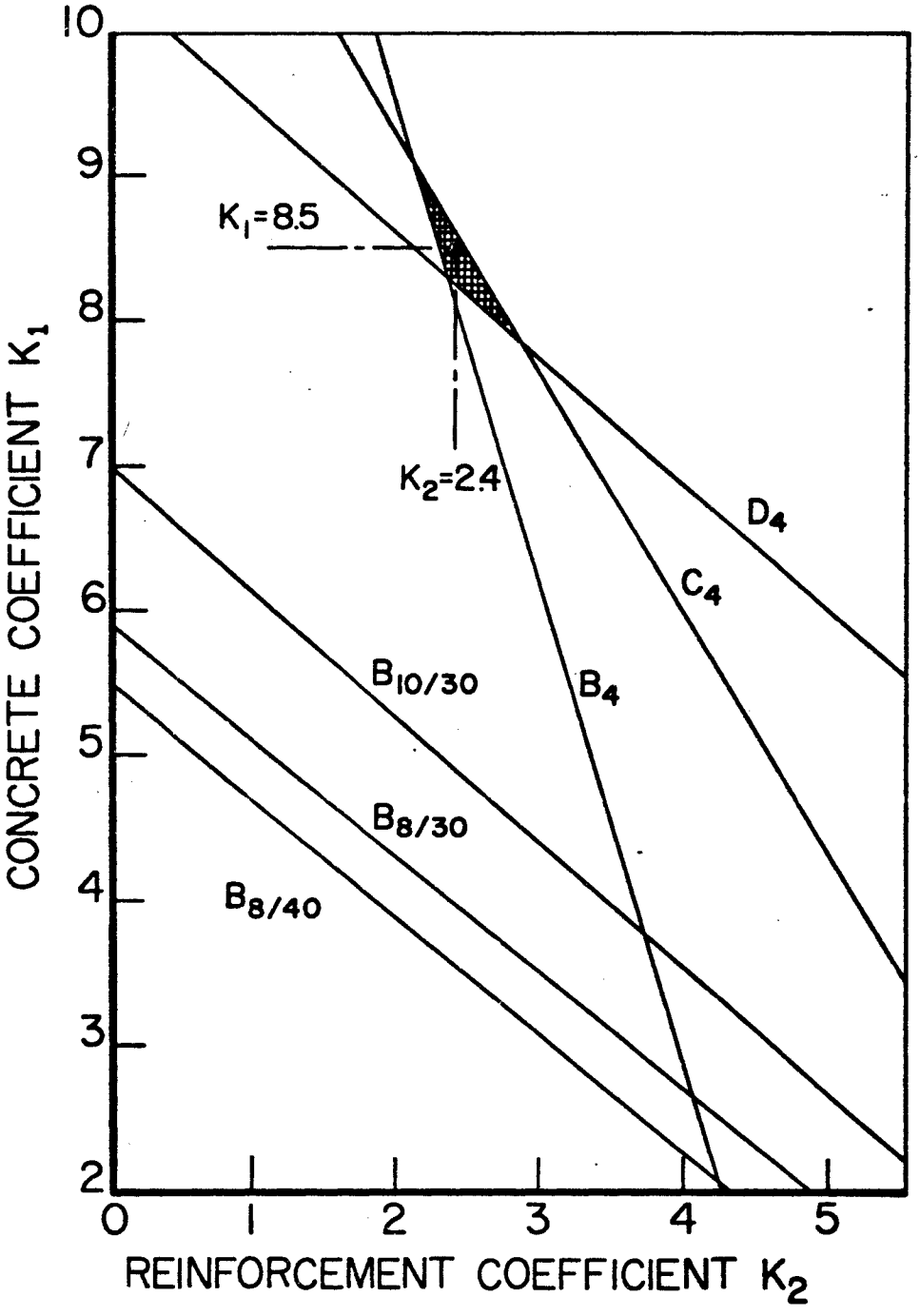

FIG. (4.6) - GRAPHICAL SOLUTION FOR K_1 AND K_2.

The ideal failure of a composite T-beam would be the simultaneous occurrance of

i) flexural failure of the concrete slab

ii) shear connector failure, and

iii) longitudinal cracking of the slab.

For such an ideal case of failure, Q_c must be equal to Q_u, where Q_u is the ultimate capacity of one shear connector. Then, from equation (4.2).

$$Q_u = 8.5\ A_{cc}\ \sqrt{U_w} + 2.4\ A_{rc}\ f_y$$

$$= 8.5\ t.S\ \sqrt{U_w} + 2.4\ A_t.S\ f_y$$

or

$$\frac{Q_u}{S} = 8.5\ t\ \sqrt{U_w} + 2.4\ A_t\ f_y \qquad \ldots\ (4.3)$$

Equation (4.3) displays the relative contribution of the concrete and reinforcement to slab shear resistance for the three half-scale T-beams tested. Davies did not suggest the equation is fully applicable to beams under real conditions of loading since such an empirical formula can be valid only within the scope of the experimental condition and accuracy. The graphical representation of equation (4.3) is shown in Fig. (2.2) using U_w = 7,000 psi.

Using equation (4.3) it is possible to estimate the amount of transverse reinforcement which would have permitted a crack to have appeared longitudinally in beam A_4 at the same time as ultimate flexure, when the load per connector was

6.92 kips. Putting the appropriate values in equation (4.3) to get:

$$A_t = 0.0205 \text{ in}^2/\text{in.}$$

then $$p = 0.82\%$$

$$pf_y = 492 \text{ psi}$$

Therefore, Davies has concluded that the minimum amount of reinforcement necessary to prohibit the development of longitudinal cracking prior to failure was found to be 0.82 per cent for the section of the test beams.

CHAPTER V

DISCUSSION OF LONGITUDINAL SHEAR FAILURE

Although both types of composite beams, discussed in the previous two Chapters, behaved fairly similarly at an early stage of loading, some differences were noticed at the longitudinal cracking load as well as at ultimate load. In addition, all tests have shown the importance of transverse slab reinforcement and the necessity for a reliable design method that gives the least amount of reinforcement required to prevent the development of longitudinal cracking. It is the object of this Chapter to point out the major differences in the behaviour of solid and ribbed slab composite beam tests and to check the adequacy of the existing design equations.

5.1 Comparison of Test Results

It is clear from Figures (3.2) and (4.2) that the slab type has influenced the load-midspan deflection curves of the two types of beam tests. The moment-deflection curves for Davies' beams did not show any discontinuity or abrupt rate of change of deflection either at the start of cracking or at any later stage of loading. The rate of change of deflection began to increase steadily at the vicinity of the cracking load. However, for all the beams with cellular metal decking

a sudden drop of load accompanied by a longitudinal crack can be noticed from Fig. (3.2). Thus, the sudden drop of load can be considered as a specific phenomena of longitudinal shear failure of composite beams incorporating metal decking. This phenomena can perhaps be explained by the following reasoning. Part of the longitudinal shear is likely to be resisted by frictional stresses present at the upper surface of the metal deck. The static frictional stress will increase the shear resistance of the lower part of the slab which has low shear capacity due to the presence of axial tensile stress at that part of the slab. When the applied load produces a shear equal to the total shearing resistance of the slab, a sudden longitudinal crack is expected to occur through the total thickness of the slab. Therefore, it is not necessary in such beams that the crack should start at the lower part of the slab and then propagate gradually up to the top surface as had been reported[3] for solid slab composite beams.

Another difference which is worth mentioning is the slip characteristics at ultimate loads. Comparing Figures (3.6) and (4.5), it can be stated that the difference between the maximum and minimum slip at any load in the in-elastic zone is comparatively small in Davies' beams as compared to the ribbed slab beams. Therefore, solid slab composite beams are expected to give better agreement than cellular slab

type as far as the assumption of equal shear forces, Q, is concerned.

Considering the empirical approach used in deriving Davies' design equation, similar equation to eq. (4.2) can be written for the beam tests incorporating cellular metal decking. Eq. (4.3) is applied for each of $B_{8/30}$, $B_{10/30}$ and $B_{8/40}$ using an equivalent cube strength as reported by Evans[9] to get:

$$\begin{aligned} 6350 &= 15K_1 \sqrt{5100} + 0.0145 \times 60000\ K_2 \\ 7000 &= 15K_1 \sqrt{4500} + 0.0145 \times 60000\ K_2 \qquad \ldots (5.1) \\ 5900 &= 15K_1 \sqrt{5100} + 0.0145 \times 60000\ K_2 \end{aligned}$$

The plot of the above three equations are shown in Fig. (4.6). From that plot, it is clear that there is no possible solution for K_1 and K_2 similar to those found by Davies. It would be more reasonable, according to the empirical method of approach, to expect the three lines to be almost identical. This is because the three beams have the same reinforcement parameters with slight change in the concrete parameters. An explanation for the actual plot of the lines can be reasoned by the existing differences in the slab width and length of the three tested beams which are believed to have a pronounced effect on the shearing resistance of the slab.

5.2 Test Results Versus Existing Design Procedures

CP 117 and Johnson, as discussed in Chapter II, have suggested empirical equations for estimating the longitudinal shear strength of the concrete slab for a given concrete strength and transverse reinforcement. Thus, this slab strength can be calculated from the recommended equations for each beam test at the start of longitudinal cracking of the slab. The comparison between the test results and the existing design procedure is made for convenience in terms of the percentage of transverse reinforcement as shown in Table (5.1). The equivelant cylinder or cube strength of concrete is interpolated using Evan's[9] data. In this Table, p represents the calculated percent transverse reinforcement which is given by the applicable design equation to achieve the shearing capacity of each beam up to the start of the first visible longitudinal cracking. The ratio(theor. p/exper. p) represents the ratio of the calculated percentage to the actual one of each beam. It is clear from this ratio that both the CP 117 and Johnson design equations give conservative estimates of the longitudinal shear capacity of the tested beams. In the same Table the calculated theoretical percentage of the transverse reinforcement required to achieve the maximum load-carrying capacity of each beam is also listed. This percentage, $(p)_u$, which is calculated

TABLE (5.1)

Comparison of the experimental and theoretical percent transverse reinforcement of the tested beams at first longitudinal cracking load, with existing theories.

BEAM	C.P. 117			JOHNSON		
	p %	$\frac{\text{theor. p}}{\text{exper. p}}$	$(p)_u$ %	p %	$\frac{\text{theor. p}}{\text{exper. p}}$	$(p)_u$ %
$B_{8/30}$	0.177	1.83	0.54	0.133	1.37	0.61
$B_{10/30}$	0.196	2.02	0.48	0.133	1.37	0.53
$B_{8/40}$	0.166	1.71	0.33	0.133	1.37	0.35
B_4	0.74	1.58	1.19	0.86	1.83	1.49
C_4	0.49	2.10	1.20	0.61	2.58	1.50
D_4	0.35	3.00	1.22	0.39	3.28	1.52

using $Q = \frac{A_s F_y}{m}$ seems to be also on the conservative side for Davies' beams. This is because Davies reported it to be 0.82% as calculated for beam A_4 in the previous chapter.

CHAPTER VI

PROPOSED DESIGN METHOD

6.1 General

A new ultimate strength design method for the transverse slab reinforcement of a composite beam is proposed. The method is based on estimating the magnitude of pf_y required which permits a crack to develop longitudinally at the same time as flexural capacity of the slab is attained. The method is then generalized to include other types of composite beam failure. The approach and analysis used herein is considered to be valid for simply supported composite beams, with solid, ribbed or haunched slab.

The proposed method of design makes use of Cowan's[10] criterion of failure and the method of construction of the relationship between v and pf_y as outlined in Reference (11).

6.2 Theory

6.2.1 Cowan and Zia Envelopes of Failure

To evaluate the strength of a member subjected to biaxial stress, one must establish a criterion of failure. Several theories of failure for concrete under combined stresses have been proposed, such as Mohr, Rankine, Coulomb and Cowan. Cowan suggested the combination of the maximum stress (Rankine's) and the internal friction theory (Coulomb's) as a dual criterion of failure for concrete.

His suggestion was based on the observation of two distinct modes of failure of concrete, cleavage and shear fracture. Cowan's failure envelope is shown in Fig.(6.1) where C_1 and C_2 are Mohr's circles representing simple tension and simple compression, respectively, and that 37 degrees is assumed to be the angle of internal friction of normal concrete.

A modification of Cowan's theory was proposed by Zia[10] in an attempt to reduce the abrupt change from pure cleavage failure to pure fracture failure. The modification is also shown in Fig.(6.1) and the resultant envelope will be identified, hereafter, as the Zia envelope.

6.2.2 The Experimental and Theoretical Work of Hofbeck, Ibrahim and Mattock[11]

The authors of Reference (11) studied the shear transfer in reinforced concrete; that is, when shear failure is constrained to occur along a plane. This type of shearing action is called "shear transfer" in order to distinguish it from that usually occurring in a reinforced concrete beam. Thirty-eight push-off specimens were tested, some with, and some without a pre-existing crack along the shear plane. A method was presented for the calculation of shear transfer strength in initially uncracked concrete based on a slightly modified version of the failure envelope proposed by Zia.

To explain how the v, pf_y relationship can be constructed[11], consider a push-off specimen of width w, thickness b' and shear plane of length d'. The stresses acting on a small element of

concrete lying in the shear plane will be as shown in Fig.(6.2), where

$$v = V/b'd'$$

$$\sigma_x = pf_y$$

$$\sigma_y = V/b'w$$

Since for a particular patterns of push-off specimen v/σ_y is constant, points on the Mohr circles; Fig.(6-2); at failure corresponding to v and σ_y will all lie on the straight line 0A inclined at angle θ to the normal stress axis, where θ is $\tan^{-1}(v/\sigma_y)$. The term (v/σ_y) is fixed by the proportions of the test specimen and is equal to w/d'. A series of circles are drawn, each tangent to the failure envelope. Where line OA cuts a circle establishes the point v, σ_y for the stress conditions at failure represented by that circle. A line is drawn through point v, σ_y and through the centre of that circle. Where this line cuts the circle diametrically opposite from point v, σ_y,fixes the point v, σ_x, that is, v, pf_y. By repeating this process for several circles, a succession of points v_u, pf_y can be obtained. A line through these points is the v_u, pf_y relationship obtained in the push-off specimen[11].

6.3 Shear Transfer Concept as Applied to the Slab of Composite Beam

Consider a transverse strip in the slab of a composite beam taken between two adjacent connectors. The forces acting on that strip are as shown in Fig.(6.3). The shear force Q,

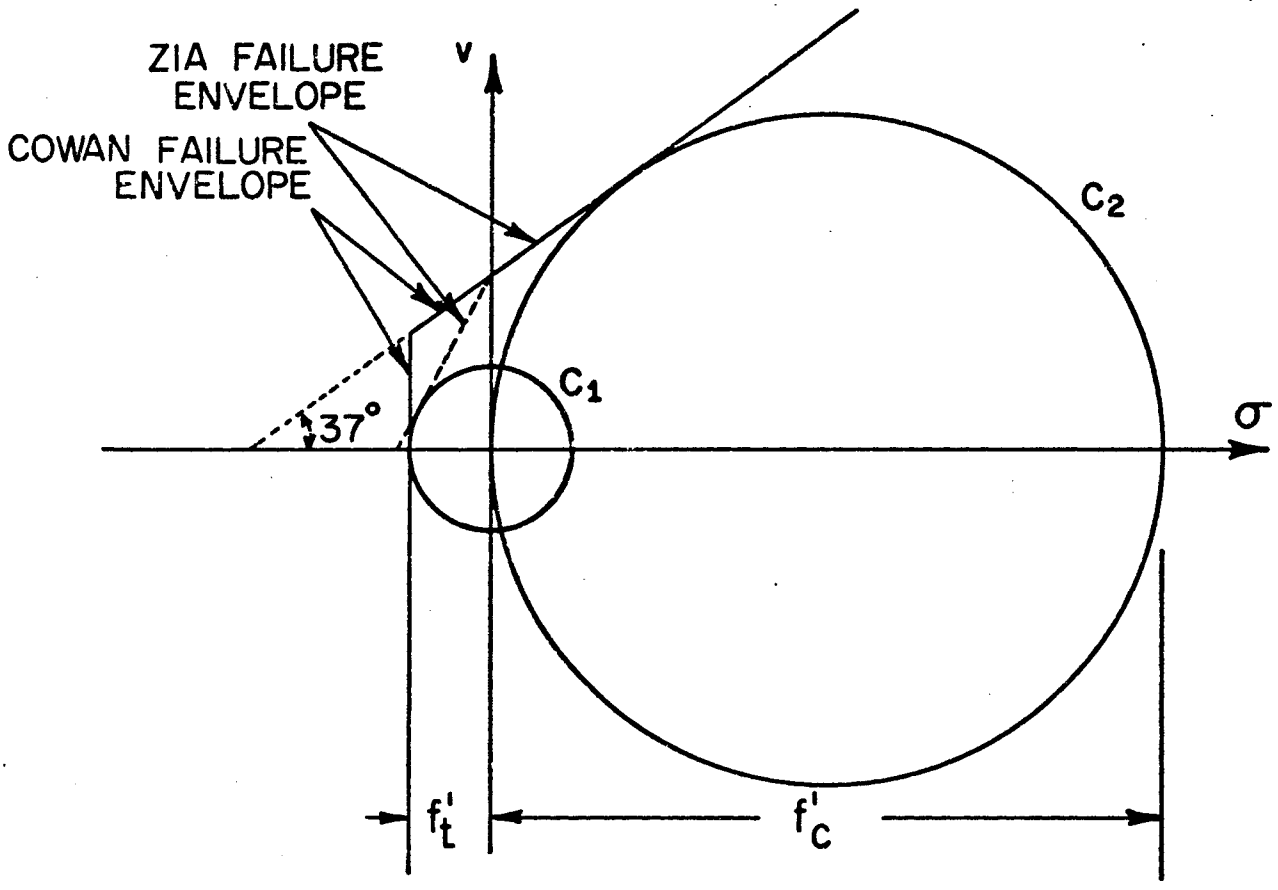

FIG. (6.1) - COWAN AND ZIA THEORIES OF FAILURE.

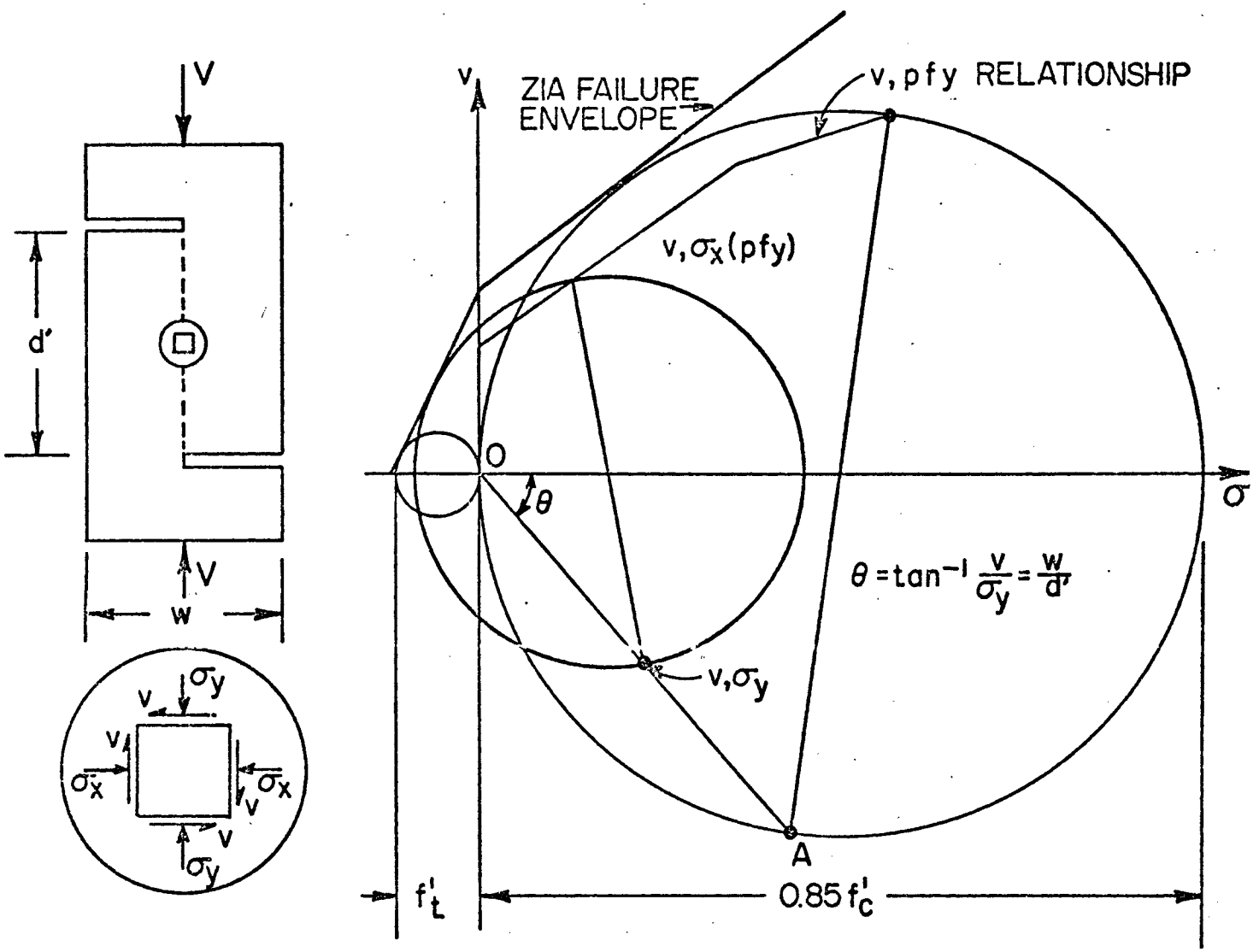

FIG. (6.2) - CONSTRUCTION OF THE RELATIONSHIP BETWEEN v AND pf_y.

which is taken to be equal in all the connectors, produces a shear stress along the two shown surfaces[1],[2],[3]. It follows that the shear failure in the strip is constrained to occur along a predetermined plane. This type of shear action has been defined in Reference (11) as a "shear transfer". In fact, a reasonable similarity exists between the strip shown in Fig.(6.3) and the push-off specimen shown in Fig.(6.2). The main differences between the two cases are the number of shear surfaces and the nature of the longitudinal stress σ_y. In the slab of a composite beam the shear plane consists of two parallel surfaces separated by the studs which run along the span. In addition, σ_y in the composite slab is produced by the bending stress which may vary in sign and magnitude throughout the thickness of the slab.

Due to the variation in σ_y throughout the slab thickness, it follows that the shear carrying capacity of concrete should vary through that thickness. That is because the former has a pronounced effect on the latter[3]. Herein, the shear stress produced by Q is considered to vary through the slab thickness and is dependent upon the shear resistance variation.

In general, two zones can be distinguished at ultimate load through and across the slab thickness. The first zone is that above the neutral axis of the slab which is under longitudinal compressive stress. The second zone is the tensile zone stress below the slab neutral axis. Both zones are shown in

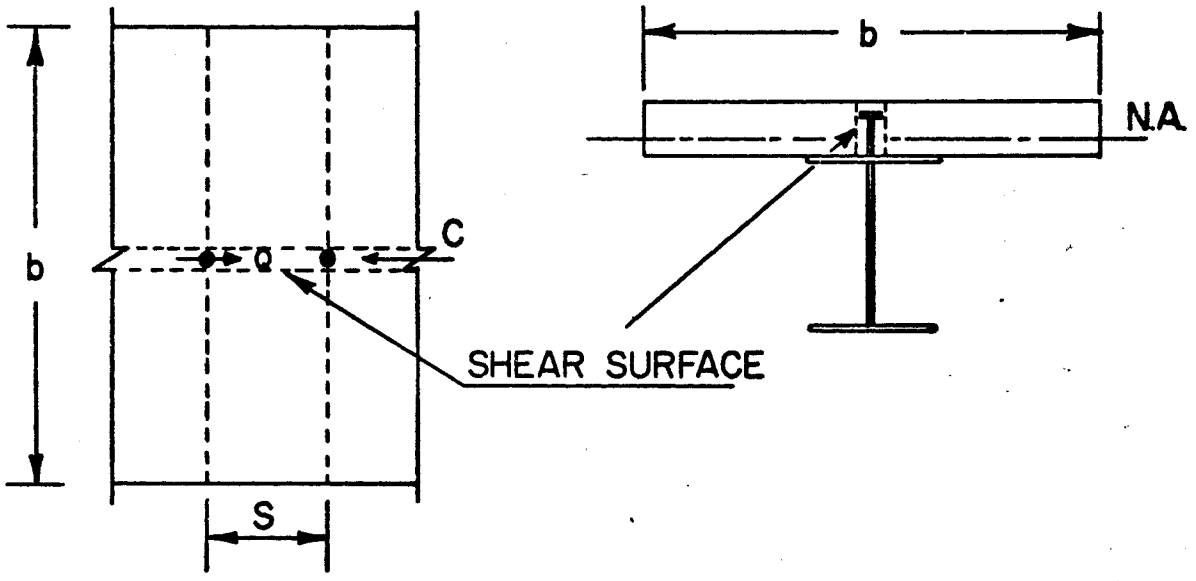

FIG. (6.3) - THE SHEAR SURFACE IN THE SLAB.

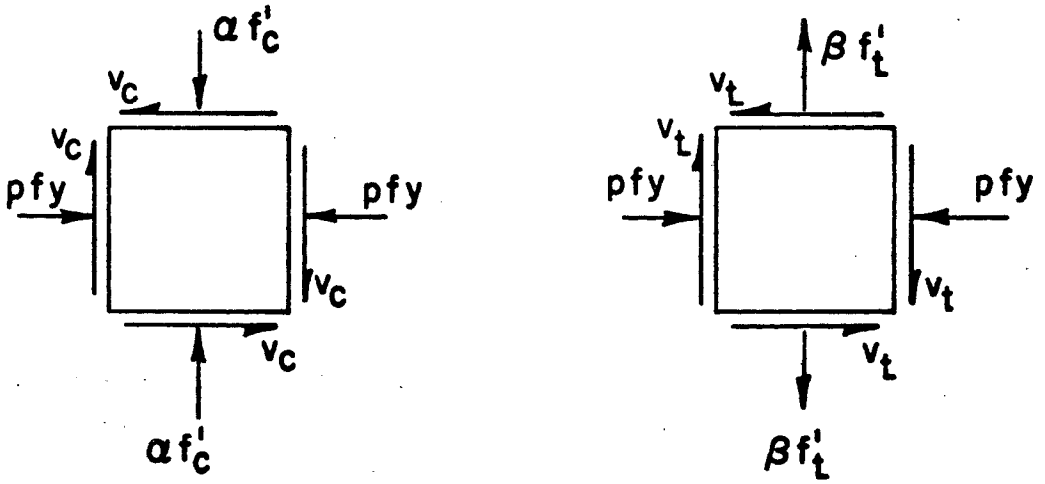

FIG. (6.4) - THE CONCRETE ELEMENTS (c) AND (t).

Fig.(6.3). Hereafter, the subscripts c and t will refer to the compressive and tensile zone respectively.

Consider two small concrete elements at the shear surface such that each one is taken from one of the two concrete zones. From the above discussion and assumptions, it follows that these elements are subjected to the stresses shown in Fig. (6.4), where,

$$\alpha f_c' = \sigma_{y_c} \quad , \quad \beta f_t' = \sigma_{y_t} \quad \text{and} \quad \sigma_x = p f_y .$$

6.4 Stress Conditions

Due to the similarity in the concrete elements of the push-off specimens of Reference (11) and the previous slab strip, the same procedure can be adopted to find the v, pf_y relation for a given element (c) of Fig.(6.4) in the composite beam slab. Fig.(6.5) shows this relation for different values of θ. For the plotted values of θ, either the Cowan or Zia envelope of failure has been used since both give identical results.

Consider the dotted curve shown in Fig.(6.5). It represents the maximum possible σ_x that would be utilized if $\alpha f_c'$ is maximum. This state is represented graphically in Fig. (6.7) for which the subscript u has been used to identify the corresponding ultimate stresses. In fact, this dotted curve can be drawn directly from Fig.(6.7) by taking several values of θ to find the associated $(\frac{v_c}{f_c'})$, and $(\frac{pf_y}{f_c'})$. It is clear that for different values of θ, the locus of these points is a circular curve

which is tangent to the $\frac{v_c}{f_c'}$ axis and having the point $(\frac{1}{2}, 0)$ as centre. This dotted curve of Fig.(6.5) is the front part of the circle of Fig.(6.7). For this circle the relation between θ and $(pf_y)_u$ can be given by:

$$(pf_y)_u = \frac{f_c'}{2} [1 - \cos 2\theta] \qquad ...(6.1)$$

It is clear from Fig.(6.2) that θ is given by:

$$\tan \theta = \frac{v_c}{\alpha f_c'} \qquad ...(6.2)$$

$$\text{then} \quad \alpha = (\frac{v_c}{f_c'}) \quad \frac{1}{\tan \theta} \qquad ...(6.3)$$

Therefore, by equation (6.3), the relation between α and pf_y at a given θ can be plotted using the corresponding values of $\frac{v_c}{f_c'}$ and $\frac{pf_y}{f_c'}$ from Fig.(6.5). This relation is shown in Fig.(6.6). The line corresponding to $(pf_y)_u$ is also shown in this figure which gives the associated values of α, i.e. α_u.

Another interesting case to study is when $pf_y = 0$. This case can be shown graphically as shown in Fig.(6.8). It follows that a state of stress exists for the concrete element (c), Fig.(6.4), in which there would be no need for any transverse reinforcement and that the element shear resistance is capable of taking the applied shear. The normal stress coefficient, α, for this case (i.e. $pf_y = 0$) is known from Fig.(6.6) for a given value of θ.

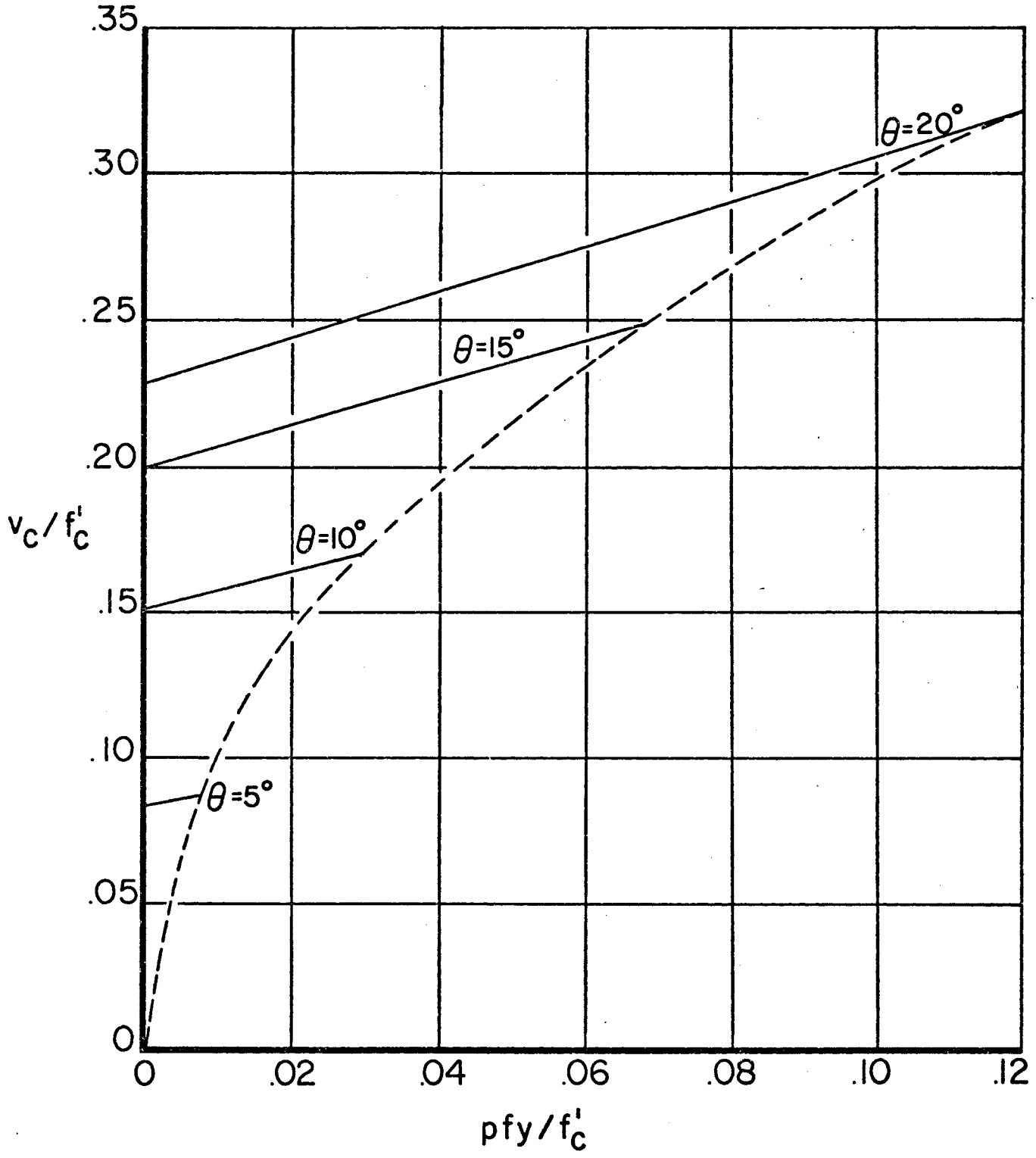

FIG. (6.5) - THE RELATIONSHIP BETWEEN v_c AND pf_y.

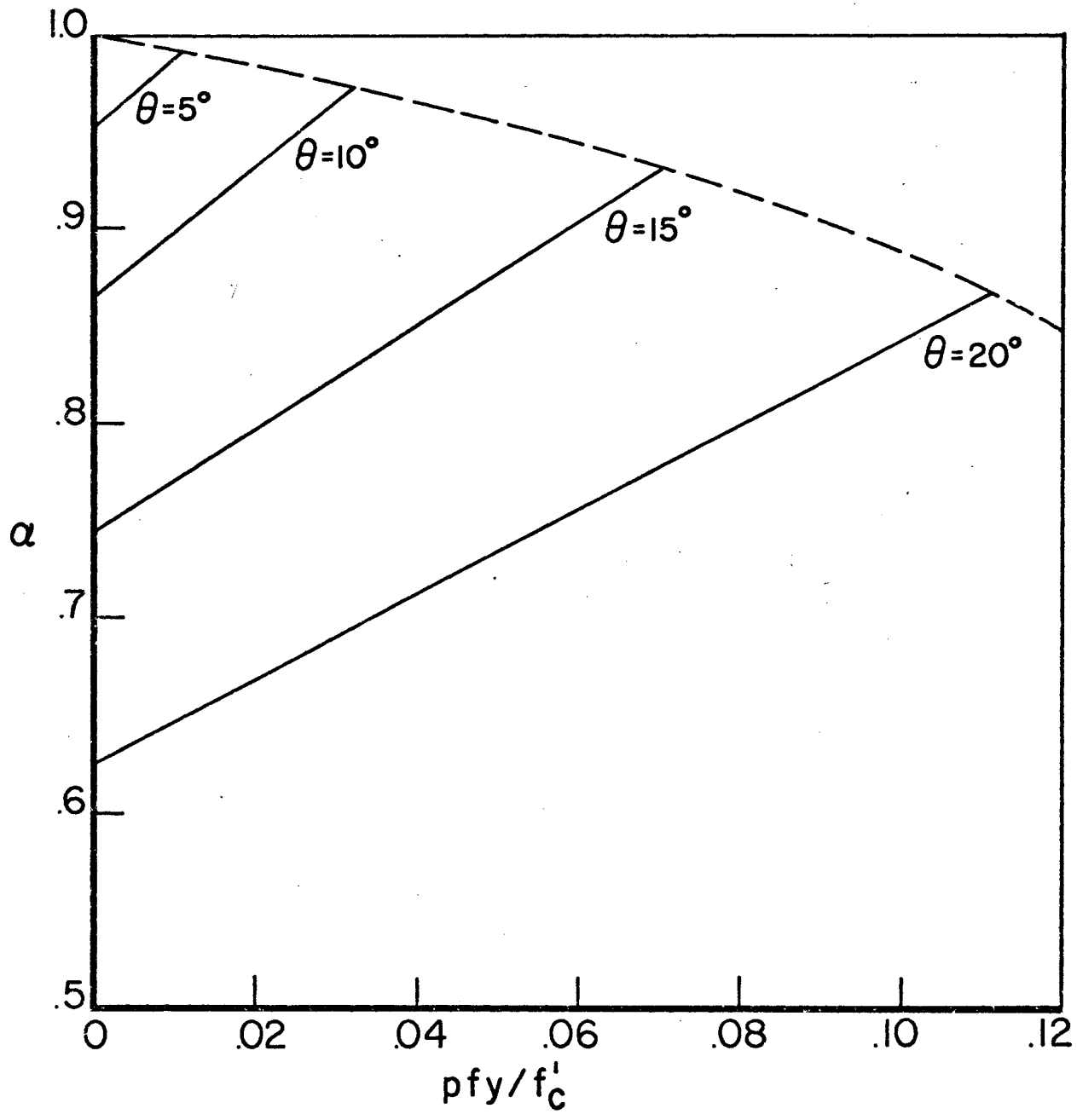

FIG. (6.6) - THE RELATIONSHIP BETWEEN α AND pf_y.

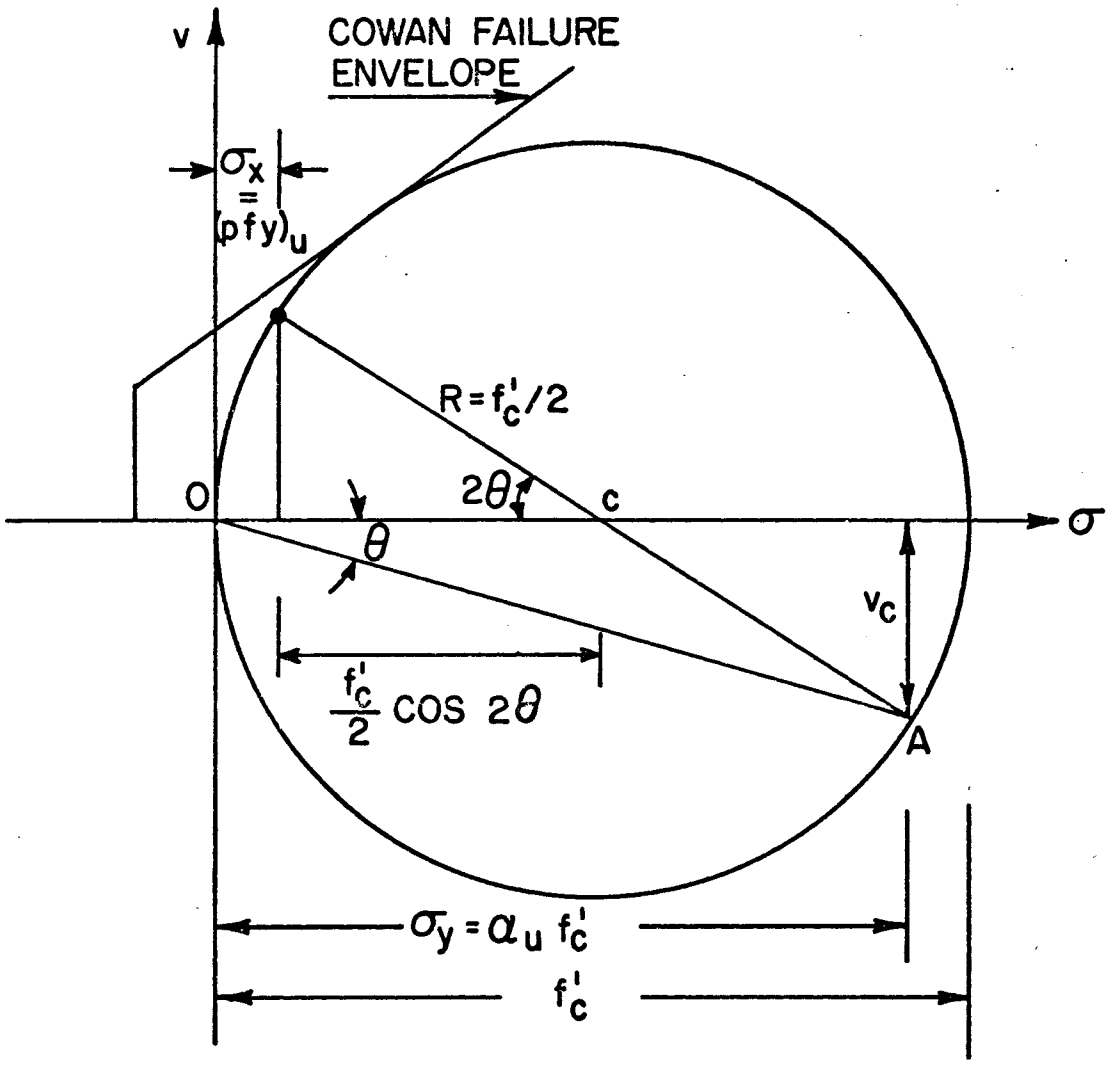

FIG. (6.7) - ULTIMATE FAILURE CONDITION.

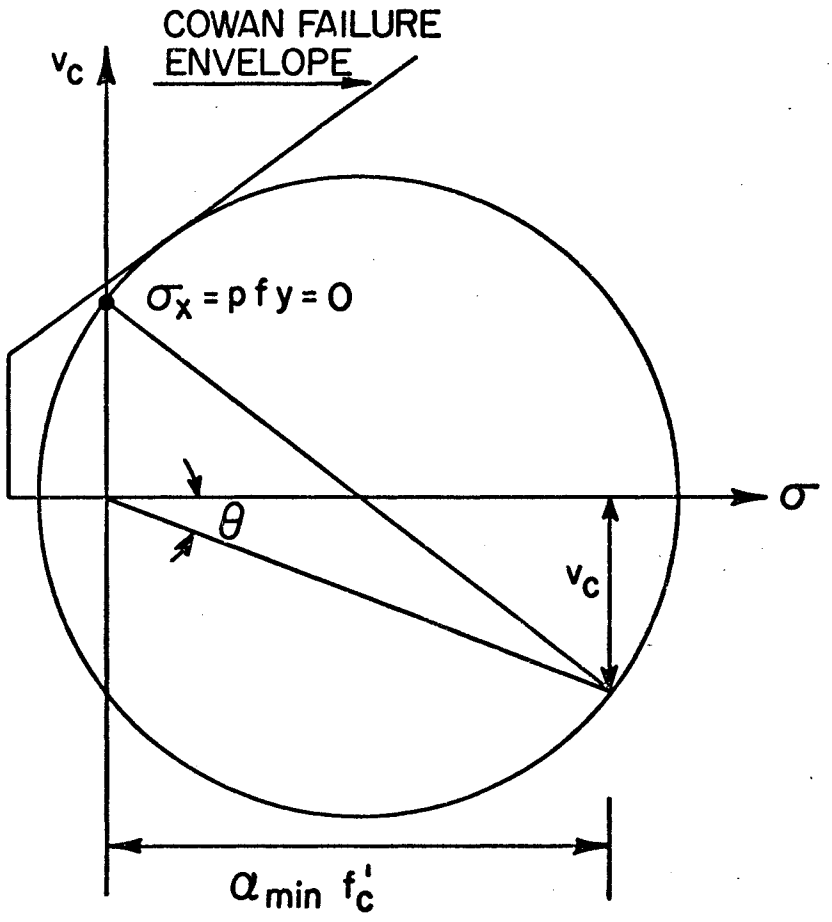

FIG. (6.8) - STRESS CONDITION FOR $pf_y = 0$.

6.5 Flexural Failure of the Slab and Associated Stresses

The flexural failure of the slab has been the most common failure of composite beam tests. In general, this failure, if not accompanied by any longitudinal or connection failure, indicates that the beam has achieved its maximum capacity. For such cases of failure, the stresses present in the most highly stressed section have been assumed as shown in Fig.(6.9). In this figure, the stress distribution is taken to be similar to that present in a reinforced concrete member. In fact, this similarity does not entirely hold true in composite beam slabs which are assumed to have vertical shear surfaces, Fig.(6.3). This is due to the existence of the longitudinal shear stress at the shear surfaces. Theoretically speaking, a concrete element will crush if it is subjected to a uniaxial stress equal to f_c'. But the element capacity would be reduced if a shear stress is applied in addition to the normal stress. To clarify this point further, consider the stresses acting on the concrete element (c) at Fig.(6.4). The maximum possible $\alpha f_c'$ that can be applied on that element was found to be given by α_u.

From Fig.(6.6) it is clear that α_u is equal to unity if, and only if, θ is zero and it decreases as θ increases. The angle θ is zero only when the applied shear stress, v_c, on the element is zero. From this it follows that the presence of shear prevents the elements from achieving their theoretical flexural capacity f_c'. In such cases, the failure of the elements

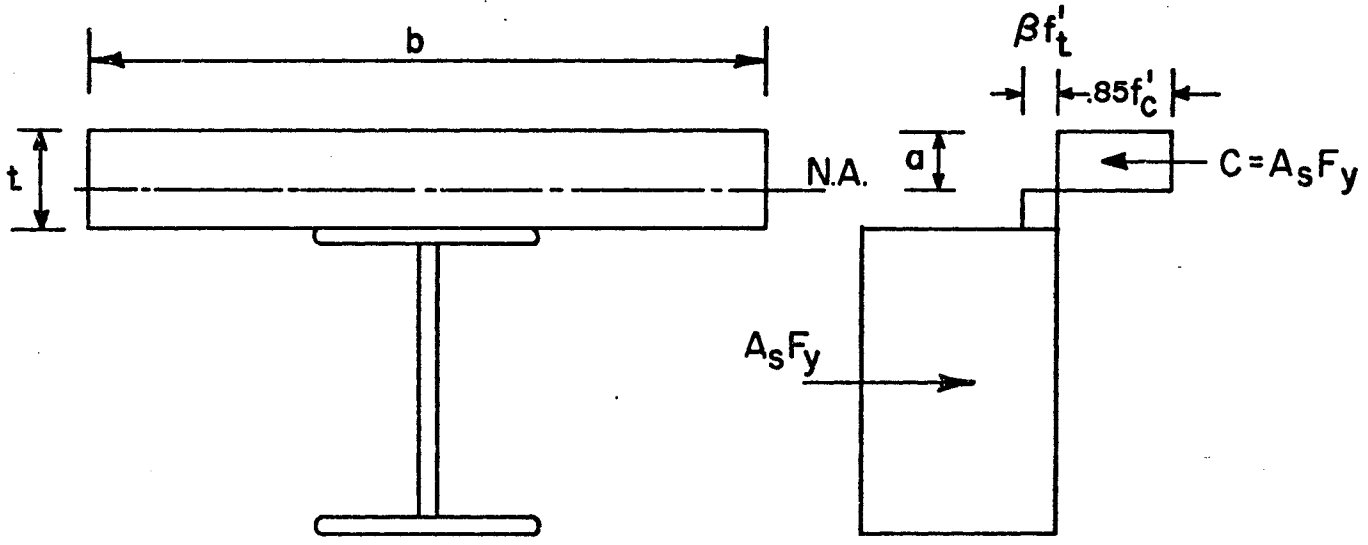

FIG. (6.9) - STRESS DISTRIBUTION ACROSS THE BEAM AT ULTIMATE LOAD.

would be of the shear-fraction type. In this type of failure, the failure plane would be along the principal plane inclined by the angle $\phi = \theta$ to the longitudinal axis of the slab. However, it is expected that the shear-fraction failure of the elements at the shear surface will be quickly followed by flexural failure of the concrete on both sides of that surface.

Therefore, and as far as the compressive part of the slab is concerned, the ultimate capacity of the concrete elements at the shear surface would be achieved when the major normal stress is $\alpha_u f'_c$. For this case, it was found that the transverse slab reinforcement should be capable of providing a stress equal to or greater than $(pf_y)_u$, and that the amount of reinforcement can be given by equation (6.1).

In Fig.(6.9), the bottom of the stress block is considered to represent also the position of the slab neutral axis. Hereafter, the part of the concrete below the distance (a) from the top fibres of the slab is assumed to be under constant tensile stress equal to $\beta f'_t$. , where,

$$a = \frac{C}{0.85 f'_c b}$$

and since for ultimate flexural capacity of the slab

$$C = \Sigma Q_u = A_s F_y$$

Then

$$a = \frac{A_s F_y}{0.85 f'_c b} = \frac{\Sigma Q_u}{0.85 f'_c b} \qquad \ldots(6.4)$$

Following the same reasoning as that used for $\alpha f_c'$, then here also β will be less than unity due to the presence of shear.

6.6 Basic Equations

Since all the elements under the same stresses have the same shear resistance, then equating the forces acting on one of the shear surfaces of the slab strip of Fig.(6.3) we get:

$$\frac{Q_u}{2} = v_c \; aS + v_t \; (t-a) \; S \qquad \ldots(6.5)$$

or

$$\frac{Q_u}{2} = v_c \; aS \; [1 + \frac{t-a}{a\rho}]$$

where $\rho = \frac{v_c}{v_t}$ represents the comparative shear resistance of elements (c) to elements (t), Fig.(6.4).

Then, $$v_c = \frac{Q_u}{2aS} \; [1 + \frac{t-a}{a\rho}] \qquad \ldots(6.6)$$

Since for the case of flexural failure of the slab we have

$$\tan \theta = \frac{v_c}{0.85 \; f_c'}$$

then, substituting in the above equation for v from equation (6.6) we get

$$\tan \theta = \frac{Q_u}{2aS} \; \frac{1}{0.85 \; f_c'} \; [1 + \frac{t-a}{a\rho}]$$

By substituting the value of a as given from equation (6.4) and cancelling the terms $0.85 \; f_c'$, we get

$$\tan \theta = \frac{Q_u}{\Sigma Q_u} \; \frac{b}{2S} \; [1 + \frac{t-a}{a\rho}]$$

or $$\tan \theta = \frac{b}{2Sm} \; [1 + \frac{t-a}{a\rho}]$$

Where $m = \frac{\Sigma Q}{Q}$ is the number of connections up to the section under consideration.

Since Sm is equal to the shear span L_v then the above equation becomes:

$$\tan \theta = \frac{b}{2L_v} \left[1 + \frac{t-a}{a\rho}\right] \qquad \ldots(6.7)$$

6.7 The Contribution of the Slab Tension Zone

Fig.(6.10) shows a general stress condition for a longitudinal shear type of failure since:

(i) the ultimate flexural failure is not achieved; $\alpha < \alpha_u$

(ii) circles c_1 and c_2 are tangent to the failure envelope.

For this case, let v_c and v_t denote the average shear stress of the top and bottom of the concrete slab respectively. It is clear from Fig.(6.10) that $v_c >> v_t$, or $\rho >> 1.0$. In fact, it is believed that ρ is not constant through the process of loading of the composite beam. It starts, say, with a value of unity until the limiting stresses of the tension zone elements are attained. Then, due to the constraint provided by the upper part of the slab, it is expected that, with the increase of load, the lower part of the slab remains in a stationary condition without longitudinal shearing. That is to say, v_t remains constant while the shear stress in the compressive zone is gradually increasing. Finally, a longitudinal crack is expected to start at the lower part of the slab as the ultimate condition of the compression zone of the slab is approached.

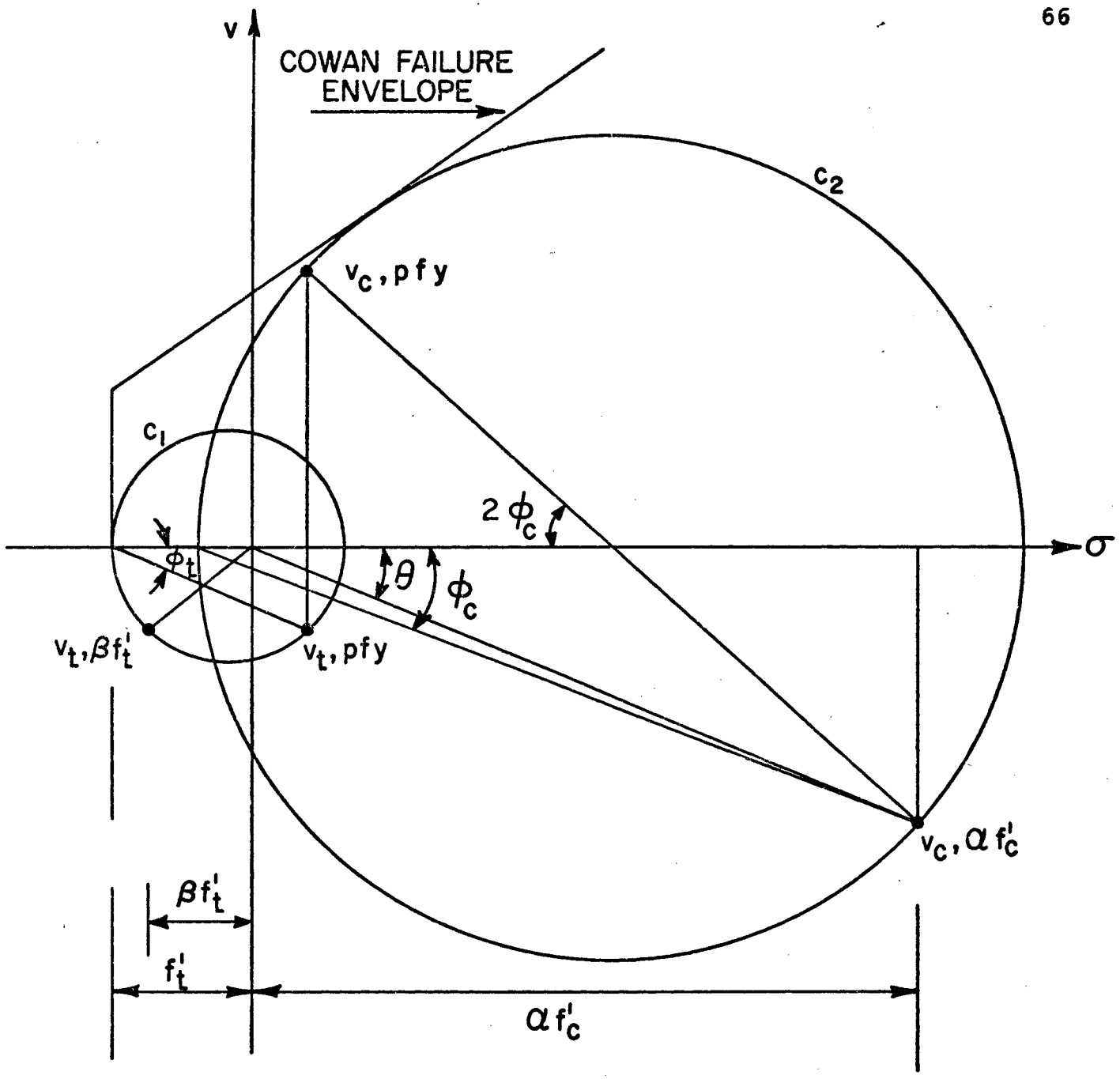

FIG. (6.10) - GENERAL STRESS CONDITION AT FAILURE.

Referring to Fig.(6.10), it seems reasonable to assume that the two principal direction ϕ_c and ϕ_t are equal prior to failure, where

$$\tan \phi_t = \frac{v_t}{f_t' + pf_y} \qquad \ldots(6.8)$$

and

$$\tan 2\phi_c = \frac{2v_c}{\alpha f_c' - pf_y} \qquad \ldots(6.9)$$

This assumption implies that the cracking surface tends to be continuous throughout the shear surface. However, if $\phi_c \neq \phi_t$ it is expected that there will be an abrupt change in the crack pattern through the thickness of the slab, and that change, if present, has to be at the slab N.A.

Thus, substituting $\phi_c = \phi_t = \phi$ into equations (6.8) and (6.9) we get:

$$v_c = \tan 2\phi \left[\frac{\alpha f_c' - pf_y}{2}\right]$$

and $$v_t = \tan \phi \left[f_t' + pf_y\right]$$

Then $$\rho = \frac{\tan 2\phi}{2 \tan\phi} \frac{\alpha f_c' - pf_y}{f_t' + pf_y} \qquad \ldots(6.10)$$

Equation (6.10) shows that ρ is a function of ϕ, α, pf_y and the concrete strength. To check the practical range of variation of ρ in composite beams consider the two extreme cases:

(i) the case when no transverse reinforcement is used, as represented in Fig.(6.8).

Substituting $pf_y = 0$ in equation (6.9) we get;

$$\tan 2\phi = 2 \frac{v_c}{\alpha f_c'}$$

but since $\tan \theta = \frac{v_c}{\alpha f_c'}$

Then

$$\tan 2\phi = 2 \tan \theta \qquad \ldots(6.11)$$

Then, for a given concrete strength and θ, the corresponding ρ is calculated from equation (6.10) by knowing ϕ from equation (6.11) and α from Fig.(6.6).

(ii) the case when ultimate capacity of the slab is achieved; i.e. when $pf_y = (pf_y)_u$.

It follows from Fig. (6.7) that $\phi = \theta$. The same procedure as above is used to find ρ for a given θ.

The relation ρ - tan θ is plotted as shown in Fig.(6.11) for concrete compressive strengths of 6,000 psi and 3,000 psi. For that plot, f_t' has been taken to be equal to $0.68 (f_c')^{3/4}$, [10]. For comparison, the two cases are shown in the figure, from which it follows that ρ decreases as θ and/or pf_y increase.

It may be seen that for the plotted range of tan θ, ρ drops to four when tan $\theta = 0.4$ and it can go up to twelve for tan $\theta = 0.1$. Then for that range of θ, the shear resistance of the tension zone of the slab is much less than that of the compression zone.

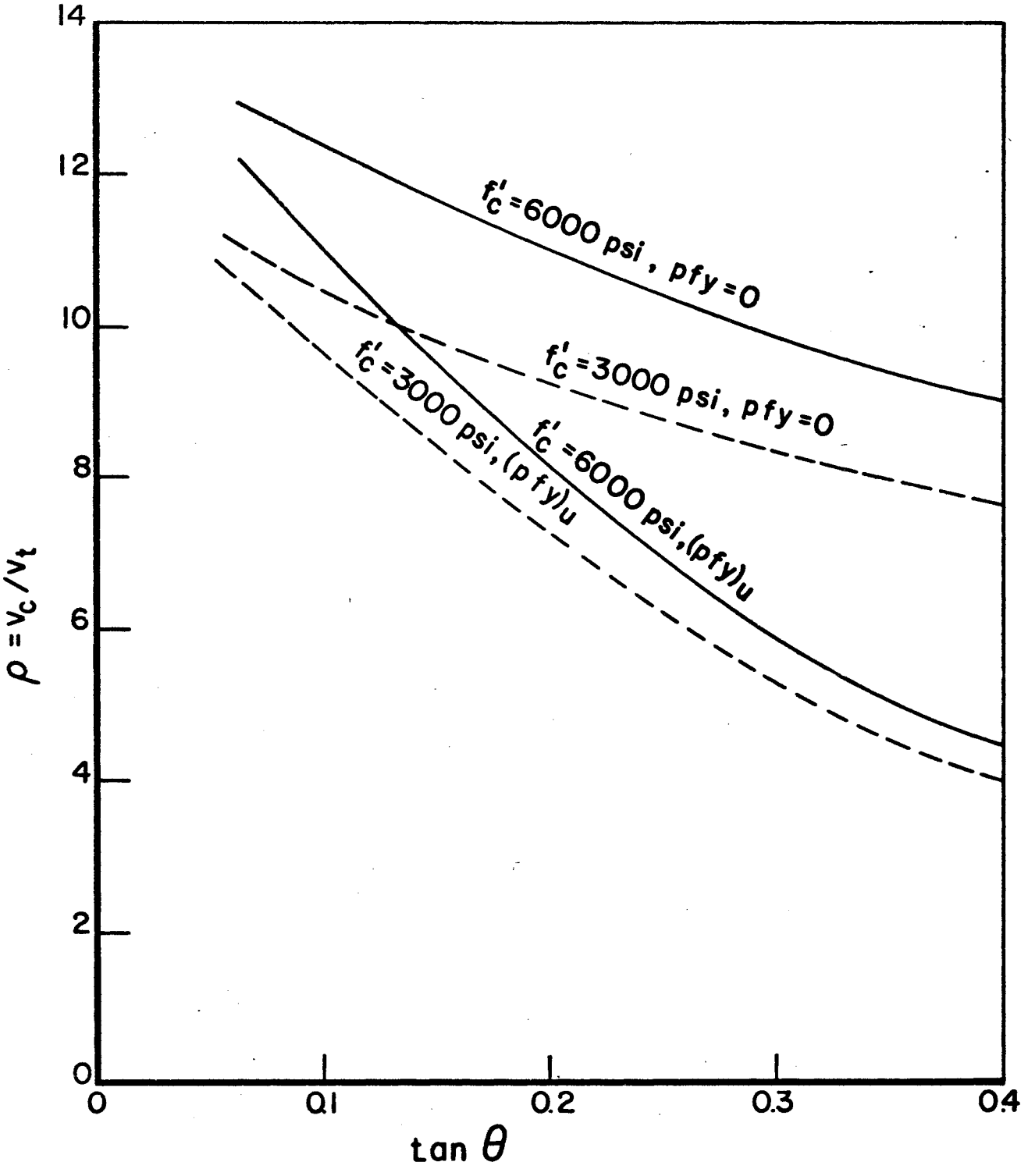

FIG. (6.11) - THE RELATIONSHIP BETWEEN ρ AND TAN θ.

Consider now the term $\frac{t-a}{a\rho}$ of equation (6.7). This term approaches zero when a = t or when ρ is large. In practice, the range of a is usually such that $\frac{t}{2} \leq a \leq t$. Therefore, it follows that $\frac{t-a}{a\rho}$ is always much less than unity and neglecting it will not affect the accuracy of tan θ in equation (6.7). Doing this, equation (6.7) can be simplified further to become

$$\tan \theta = \frac{b}{2L_v} \qquad \ldots(6.12)$$

6.8 Ultimate Strength Design Equation and Chart:

From all the previous discussion, it follows that the equation

$$(pf_y)_u = \frac{f'_c}{2} (1 - \cos 2\theta)$$

gives the minimum amount of transverse reinforcement required to achieve the ultimate capacity of the concrete slab. In this equation

$$1 - \cos 2\theta = 2 \sin^2 \theta$$

and since $\tan \theta = \frac{b}{2L_v}$ then $\sin \theta = \frac{b}{\sqrt{b^2 + (2L_v)^2}}$

Therefore the design equation becomes

$$(pf_y)_u = \frac{f'_c}{1 + \left(\frac{2L_v}{b}\right)^2} \qquad \ldots(6.13)$$

If $(\frac{pf_y}{f_c})_u$ is plotted against $\frac{b}{2L_v}$, equation (6.13) would be represented graphically as a circular curve similar to the dotted curve of Fig. (6.5). This plot is shown in Fig. (6.12) which is the design chart of the proposed ultimate strength design.

For the case when the plastic neutral axis is within the steel beam, the same adopted procedure is still applicable. But, in this latter case, the sum of the connection shear forces, ΣQ, at flexural failure of the slab would be given by,

ΣQ = the ultimate compression capacity of the slab

= $0.85\ f'_c\ bt$.

6.9 Other Types of Composite Beam Failure

Consider now a composite beam which has transverse slab reinforcement less than that required to achieve the ultimate flexural capacity of the slab; i.e. $pf_y < (pf_y)_u$. In this case, a longitudinal crack is expected to occur at the most stressed section in the slab, then to develop towards the supports as the load increases. At this section of the slab, it is rather difficult to predict the exact stress distribution when the longitudinal crack starts. However, an approximation of the bending stress distribution likely to be present above the section neutral axis is shown in Fig.(6.13). This approximation is based on elastic-plastic type of stress distribution since the ultimate flexural condition of the slab has not been attained. The

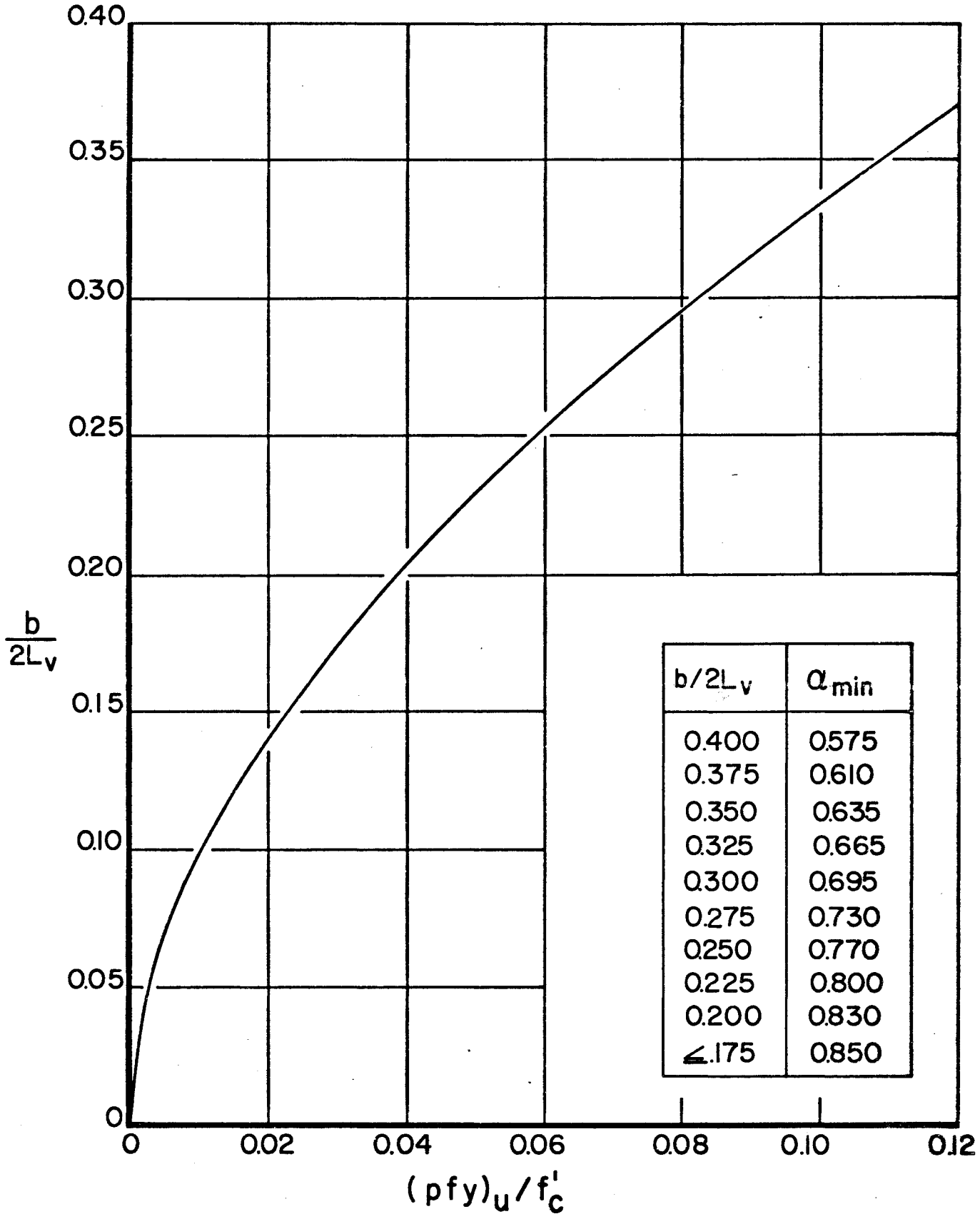

FIG. (6.12) - THE PROPOSED ULTIMATE STRENGTH DESIGN CHART.

position of the neutral axis is also considered in this type of failure to be given by the distance a from the slab top fibres, where

$$a = \frac{A_s F_y}{0.85\ f_c' b} \qquad \ldots(6.14)$$

In fact, the position of the neutral axis in a reinforced concrete section tends to propagate up while the ultimate condition is being approached. However, the range of variation of the neutral axis between elastic and plastic stages of loading is rather small and it has been neglected.

Using the same reasoning here as that used for disregarding the tension zone contribution, then, the longitudinal shear is considered to be taken by the part of the slab above the neutral axis. Although the longitudinal normal stress varies through the slab thickness, it is assumed that all the concrete elements at the shear surfaces will fail simultaneously when their total shearing resistance is utilized. It follows from Mohr circles representing failure conditions in Figs.(6.7) and (6.8) that the transverse normal stress, σ_x, varies through the slab thickness since it is dependent upon the magnitude of the longitudinal normal stress $\alpha f_c'$. The variation of σ_x is such that

(i) when $\alpha f_c' = \alpha_u f_c'$; $\sigma_x = (pf_y)_u$

(ii) when $\alpha f_c' \leq \alpha_{min} f_c'$; $\sigma_x = 0$

The above two cases represent the failure of the concrete elements above y and below γa of Fig. (6.13) respectively. For the intermediate concrete elements within x, the transverse stress would be somewhere between zero and $(pf_y)_u$. For simplicity and in order to be on the conservative side, this intermediate zone is included with the one above it resulting in a transverse stress of $(pf_y)_u$ utilized within γa prior to failure of the beam in question. Then the total transverse force utilized prior to failure of the part of the slab above the neutral axis is given by $(pf_y)_u \gamma a$ per unit length of the slab. This transverse force results in an average stress of $(pf_y)_u \frac{\gamma a}{a}$ which should equal the average transverse stress produced by the reinforcing bars throughout the slab thickness. The latter average transverse stress is assumed to be acting throughout the total thickness of the slab regardless of the position of the transverse reinforcing bars in the slab.

Thus ,

$$p'f_y = (pf_y)_u \quad \gamma \qquad \ldots(6.15)$$

where p' is the steel ratio in the concrete slab for partial ultimate capacity.

The coefficient γ in the above equation is a function of the stress distribution shown in Fig. (6.13), and a general

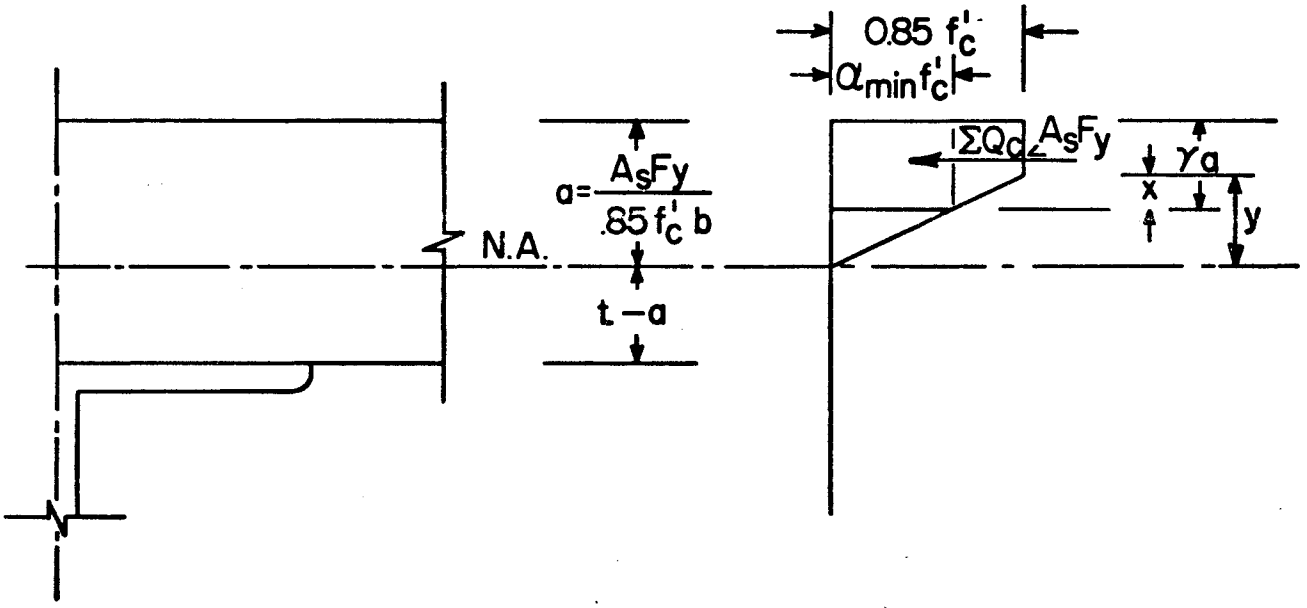

FIG. (6.13) - EFFECTIVE BENDING STRESS DISTRIBUTION IN THE SLAB FOR PARTIAL ULTIMATE STRENGTH.

expression for it can be derived as follows:

$$\gamma a = a - y + x$$

$$\text{or} \quad \gamma = 1 - \frac{y - x}{a} \qquad \ldots(6.16)$$

from similar triangles we get:

$$\frac{y - x}{y} = \frac{\alpha_{min}}{0.85}$$

$$\text{or} \quad y - x = y \frac{\alpha_{min}}{0.85}$$

Substituting the above value of (y - x) into equation (6.16), we get,

$$\gamma = 1 - y \frac{\alpha_{min}}{0.85a} \qquad \ldots(6.17)$$

An expression for y can be found by equating the total force due to bending in the slab to C,

$$\text{i.e.} \quad C = 0.85 f_c' b \left(a - \frac{y}{2}\right) \quad ; \quad C < A_s F_y$$

$$\text{or} \quad y = 2 \left(a - \frac{C}{0.85 f_c' b}\right)$$

Substituting y into equation (6.17), we get,

$$\gamma = 1 - \frac{2 \alpha_{min}}{0.85a} \left(a - \frac{C}{0.85 f_c' b}\right)$$

$$\text{or} \quad \gamma = 1 - 2.35 \alpha_{min} \left(1 - \frac{C}{0.85 f_c' ba}\right)$$

and since $a = \frac{A_s F_y}{0.85\, f'_c b}$

then $\gamma = 1 - 2.35\, \alpha_{min} \left(1 - \frac{C}{A_s F_y}\right)$ ...(6.18)

Finally, substituting γ into equation (6.15), we get

$$p'f_y = (pf_y)_u \left[1 - 2.35\, \alpha_{min} \left(1 - \frac{C}{A_s F_y}\right)\right] \quad ...(6.19)$$

The above equation implies that for a given $(pf_y)_u$, α_{min} and $A_s F_y$ then C and hence the moment at first longitudinal cracking can be determined for any value of the transverse slab reinforcement parameter, $p'f_y$. $(pf_y)_u$ and α_{min} can be known for a given $\frac{b}{2L_v}$ from Fig.(6.12) in which the corresponding values of α_{min} as found from Fig.(6.6) are tabulated.

Equation (6.19) can be re-arranged to give

$$C = A_s F_y \left\{1 - \frac{1}{2.35\, \alpha_{min}} \left[1 - \frac{pf_y}{(pf_y)_u}\right]\right\}$$

and since $C = \Sigma Q_c = m\, Q_c$

then $Q_c = \frac{A_s F_y}{m} \left\{1 - \frac{1}{2.35\, \alpha_{min}} \left[1 - \frac{pf_y}{(pf_y)_u}\right]\right\}$ ...(6.20)

Another feature of equation (6.19) is that it can be used to determine the minimum amount of transverse slab reinforcement required when there is only partial connection. This type of failure is likely to occur when $\Sigma Q_u < A_s F_y$, where Q_u is the ultimate shearing strength of a connector. In fact

in this case also, the same elastic-plastic stress distribution shown in Fig. (6.13) can be considered valid at the connection failure. As a result, equation (6.19) would be in this case:

$$p'f_y = (pf_y)_u \left[1 - 2.35\, \alpha_{min} \left(1 - \frac{\Sigma Q_u}{A_s F_y}\right)\right] \qquad \ldots(6.21)$$

where $p'f_y$ here represents the transverse reinforcement parameter required for the simultaneous occurrence of shear connection failure and the excessive longitudinal cracking of the slab.

CHAPTER VII

COMPARISON AND CONCLUSION

7.1 Comparison with Davies Test Results

In part 2 of his paper[11] "Test on half-scale steel-concrete composite beams with welded stud connectors", Davies studied the effect of transverse slab reinforcement on the behaviour and performance of composite beams. He reported the cracking loads and shear forces of Series 2 beams; A_4, B_4, C_4, and D_4; in which the transverse reinforcement was reduced in successive beams.

The cube strength and the equivalant cylinder strength of concrete for all the beams are listed in Table (7.1). The equivalant cylinder strength was made using Evan's Table[9] of conversion. The table also shows a comparison between the experimental pf_y and connector force at cracking Q_c as reported by Davies and the associated theoretical values calculated using the proposed design equations. The theoretical values of pf_y were found by substituting the shear forces as reported by Davies into equation (6.19), whereas equation (6.20) and the actual pf_y were used for the calculation of the theoretical Q_c. In these two equations, α_{min} was taken to be 0.68 as given by Fig. (6.12). The flexural failure of beam A_4 was not accompanied by any longitudinal cracking along the line of the

shear connectors. This beam was excluded from the theoretical calculation since its slab proved to be transversly over-reinforced.

It is clear from comparing the two values of pf_y of each beam that the theoretical values are in good agreement with the actual pf_y used. It is also clear that the difference between the experimental and theoretical values increases with the decrease of pf_y having a maximum of 9.2% for beam C_4 and a minimum of - 22.5% for beam D_4. However, an excellent agreement of the theoretical and the experimental values of Q_c exists for all the beams with a maximum difference of less than $\mp$ 4.5%.

Davies also reported that the shear resistance per inch run of beam could be represented by the following empirical expression:

$$\frac{Q_u}{S} = 8.5\ t\sqrt{U_w} + 2.4\ A_t f_y$$

Using the above expression, Davies reported that the amount of transverse reinforcement which would have permitted excessive longitudinal cracking in beam A_4 at the same time as ultimate flexure would be 0.0205 in^2/in. This is equal to 0.82 per cent resulting in a pf_y value of 492 psi when f_y is 60,000 psi. Almost the same reinforcement can be obtained by putting the appropriate values of f_c' and $b/2L_v$ into equation (6.13). The calculated $(pf_y)_u$ value from this equation is 490 psi which by definition would permit a crack

to develop longitudinally as ultimate flexure is attained.

It follows from the above comparison that the proposed theoretical approach is in good agreement with Davies tests and his empirical equation. The agreement is almost perfect in the predicted transverse reinforcement and the shear force for the full ultimate condition. In addition the calculated values of Q_c for Davies beams are almost identical with the experimental ones. As a result, the compressive force C in the slab due to bending can be estimated for any amount of transverse slab reinforcement. Knowing C, then the applied moment for the case of partial ultimate failure can be calculated.

Referring to Davies empirical expression, it is possible to derive a similar expression using the theoretical values obtained by assuming any two distinct values of pf_y. Let these two values be the upper and lower limits of pf_y; i.e. $(pf_y)_u$ and zero; and A_sF_y and v_u be as those given for beam A_4. Then, equation (6.20) gives

$$Q_{c1} = 2.6 \text{ kip} \qquad \text{for } pf_y = 0$$

and

$$Q_{c2} = 6.92 \text{ kip} \qquad \text{for } (pf_y)_u = 490 \text{ psi}$$

Then the concrete coefficient K_1 would be given by

$$K_1 = \frac{Q_{c1}}{t.s\sqrt{U_w}} = 8.80$$

and the reinforcement coefficient K_2 would be

$$K_2 = [\frac{Q_{c2}}{t.S} - K_1 \sqrt{U_w}]/(pf_y)_u$$

$$= 2.35$$

The resultant expression would be

$$\frac{Q_u}{S} = 8.80t \sqrt{U_w} + 2.35 A_t f_y$$

Although the above equation is quite similar to Davies', it is valid only for the special case when $b/2L_v$ is equal to 0.312. That is because the two calculated values of either Q_c or pf_y as discussed in the proposed analysis are functions of the concrete strength and θ where $\theta \simeq \tan^{-1} b/2L_v$.

TABLE (7.1)

Comparison with Davies beam tests

Beam	U_w psi	f'_c psi	$\frac{b}{2L_v}$	experimental		theoretical	
				pf_y psi	Q_c kip	pf_y psi	Q_c kip
A_4	6,200	5,500	0.312	564	6.92	-	-
B_4	7,300	6,850	0.312	282	5.15	276	5.18
C_4	7,300	6,850	0.312	141	4.03	154	3.94
D_4	6,500	6,000	0.312	71	3.14	55	3.28

TABLE (7.2)

Comparison with cellular slab composite beam tests

Beam	$\frac{b}{2L_v}$	experimental		theoretical			
		pf_y psi	Q_c kip	pf_y psi	Q_c kip	$(pf_y)_u$ psi	p_u %
$B_{8/30}$	0.267	58	6.35	30	7.10	298	0.50
$B_{10/30}$	0.333	58	7.00	77	6.53	406	0.67
$B_{8/40}$	0.200	58	5.90	18	7.21	172	0.29

7.2 Comparison with the Composite Beam Tests Incorporating Cellular Decking

The relative differences between the behaviour and performance of solid and cellulor slab composite beam tests were mentioned and discussed in Chapter V. In that discussion, the effect of the slip and the presence of the metal deck in the latter type were shown to have a pronounced effect on the longitudinal shear resistance of the ribbed slab. In the proposed analysis, complete connection was assumed to exist between the concrete slab and the steel beam, as a result of which the slip effect, if present, was neglected. Such an assumption is believed to be violated for the three beam tests in question especially in the inelastic stage of loading. The slip, as reported by Davies, increases with the decrease in percent of transverse reinforcement in the slab which was very small in the beams $B_{8/30}$, $B_{10/30}$ and $B_{8/40}$. The presence of the metal deck adds another problem in estimating the actual stresses at failure in order to check the applicability of the proposed method to the test beams.

Table (7.2) shows the comparison between the experimental and theoretical values of pf_y and Q_c. The theoretical values are calculated as explained in the previous section. The comparison shows some uncertainty in the prediction of the actual behaviour of the beams as reflected in the range of the errors. For beams $B_{8/30}$ and $B_{8/40}$, the theory predicted

better performance than that actually observed as reflected in the magnitudes of Q_c. On the other hand $B_{10/30}$ surpassed the theoretical expectation. It is believed that a better agreement between experimental and theoretical values would have been achieved if a greater amount of transverse reinforcement had been used in the slab of the tested beams. In the same Table, the theoretical values of $(pf_y)_u$ and the corresponding percent transverse reinforcement required to achieve the ultimate flexure of the beams are listed. Although these ultimate values range from 300 to 700 percent of the values used in the beam tests, they are still close to those resulting from other design procedures[1][2] as listed in Table (5.1).

7.3 Conclusions

Since the longitudinal shear failure of the slab of composite beams is constrained to occur at a predetermined shear surface, the shear transfer concept[11] can be used to analyse the stresses on the concrete elements located at that surface. Using the Cowan or Zia envolope of failure and the method of construction of the v, pf_y relationship of reference (11) a method of analysis of these stresses is proposed. The method implies that the longitudinal shear cracking of the slab is the result of achieving the ultimate shear capacity of a concrete element which is in turn a function of the normal stresses present at the shear surface. In the analysis, the contribution of the concrete elements subjected to tensile longitudinal

stress due to bending is found to be small and it has been neglected. In addition the longitudinal compressive stress as well as the slab width and the shear span of the beam are found to be the main parameters which can not be neglected when estimating the longitudinal shear capacity of the slab.

A design chart based on estimating the transverse normal stress, $(pf_y)_u$, required within the concrete slab to achieve the full ultimate flexural capacity of the composite beam is proposed. Alternatively, using elastic-plastic stress distribution across the concrete slab, the longitudinal compressive force due to bending and hence the applied moment can be predicted for any longitudinal shear capacity of the slab.

The proposed design and analysis when compared to previous tests and analysis[3] showed good agreement between both the values of the shear force Q_c prior to failure, and in the estimated percentage of transverse reinforcement.

REFERENCES

1. British Standards Institution, Code of Practice CP 117, Part 1:1965: Composite construction in structural steel and concrete.

2. Johnson, R.P., "Longitudinal shear strength of composite beams", ACI Journal, Proceedings Vol. 67, June 1970, pp. 464-466.

3. Davies, C., "Tests on half-scale steel-concrete composite beams with welded stud connectors", The Structural Engineer, Vol. 47, No.1, Jan. 1969, pp. 29-40.

4. Yam, L.C.P. and Chapman, J.C., "The inelastic behaviour of simply supported composite beams of steel and concrete", Proc. I.C.E., Paper No.7111, Dec. 1968.

5. Canadian Institute of Steel Construction, "Handbook of Steel Constructions", 1971.

6. American Institute of Steel Construction, "Manual of Steel Construction", 1970.

7. American Concrete Institute, "Building Code Requirements for Reinforced Concrete (ACI 318-71)", 1971.

8. ACI - ASCE Committee 326, "Shear and diagonal tension", Journal ACI, Vol. 59, January, February, March 1962, pp. 1-30, 277-333, 353-396.

9. Neville, A.M., "Properties of Concrete", New York, John Wiley & Sons, Inc., 1963.

10. Zia, P., "Torsional strength of prestressed concrete members", ACI Journal, Proceedings Vol. 57, No.10, April 1961, pp.1337-1360.

11. Hofbeck, J.A., Ibrahim, I.O. and Mattock, A.M., "Shear transfer in reinforced Concrete", ACI Journal, Proceedings Vol. 66, No.2, February 1966, pp.119-128.